Flux Tubes and Confinement in Lattice Quantum Chromodynamics

Leonardo Cosmai

INFN

ICSC
Centro Nazionale di Ricerca in HPC,
Big Data and Quantum Computing

QCD Vacuum Structure and Confinement, Naxos, 28 August 2024

Outline

- Introduction
- Flux Tubes in SU(3) pure gauge at T=0
- Flux Tubes in SU(3) pure gauge at T≠0
- Flux Tubes in (2+1)-flavor QCD at T=0
- Conclusions

50 YEARS OF QUANTUM CHROMO DYNAMICS

~ 1973

QCD

$$\mathcal{L} = \sum_q \bar{\psi}_{q,a}(i\gamma^\mu \partial_\mu \delta_{ab} - g_s \gamma^\mu t^C_{ab} \mathcal{A}^C_\mu - m_q \delta_{ab})\psi_{q,b} - \frac{1}{4} F^A_{\mu\nu} F^{A\,\mu\nu}$$

- *"A Tool Supporting Experimental Exploration"*
- *"A Tool for Astrophysics and Nuclear Technology"*
- *"A pointer to New Realities"*

(Frank Wilczek, arXiv:2403.06038v1)

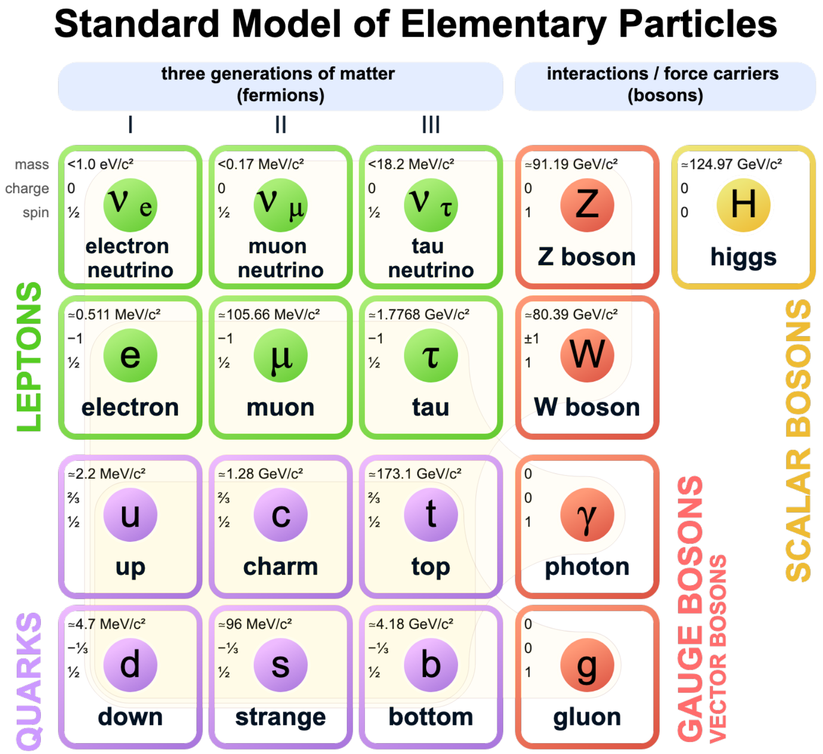

QUANTUM CHROMO DYNAMICS

$$\mathcal{L} = \sum_q \bar{\psi}_{q,a}(i\gamma^\mu \partial_\mu \delta_{ab} - g_s \gamma^\mu t^C_{ab} \mathcal{A}^C_\mu - m_q \delta_{ab})\psi_{q,b} - \frac{1}{4} F^A_{\mu\nu} F^{A\,\mu\nu}$$

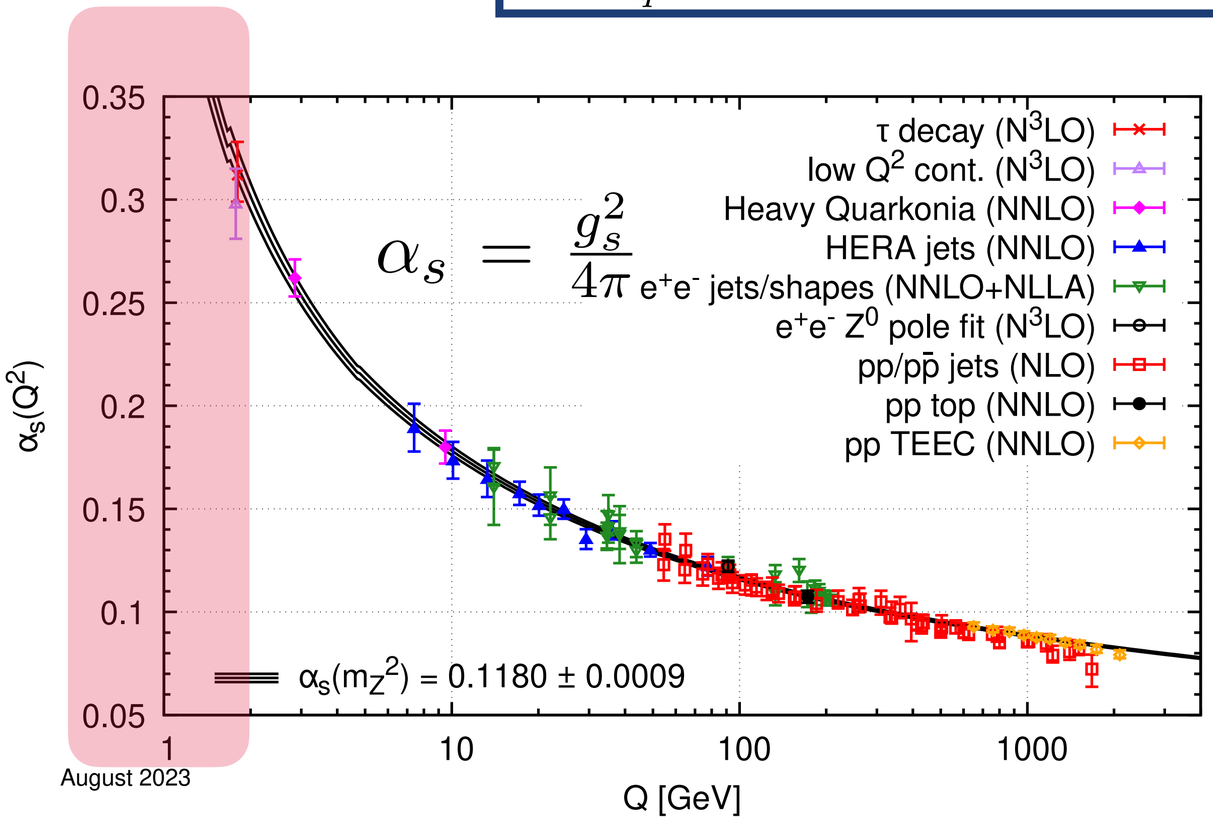

space-time discretisation

K. Wilson, 1974

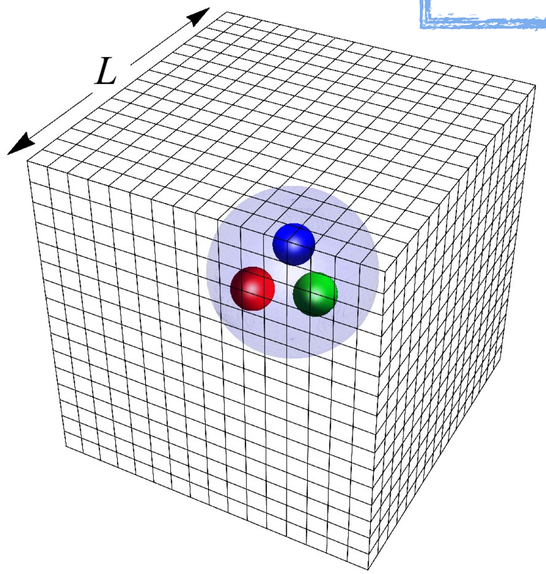

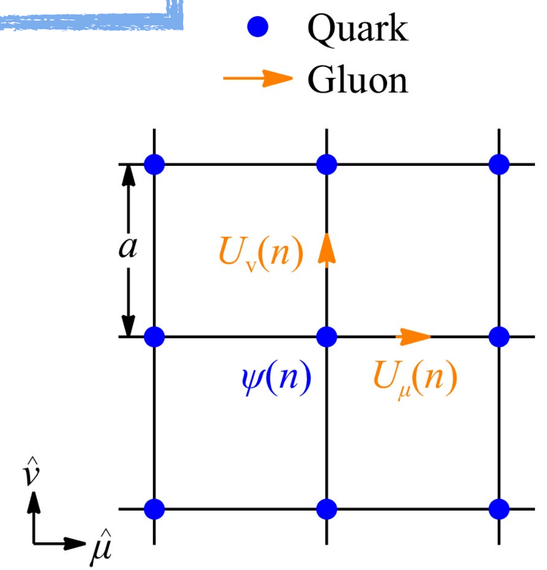

nonperturbative methods are necessary to explore the low-energy region of QCD

Lattice Quantum Chromodynamics (LQCD) provides a first-principles nonperturbative approach

Confinement of quarks and QCD on spacetime lattices

- An important empirical aspect of QCD is that only color-singlet hadrons are observed in nature.

Kenneth Wilson demonstrated (in the strong coupling limit) that SU(3) Yang-Mills theory produces an attractive potential that increases linearly with the distance between quarks, effectively confining them.

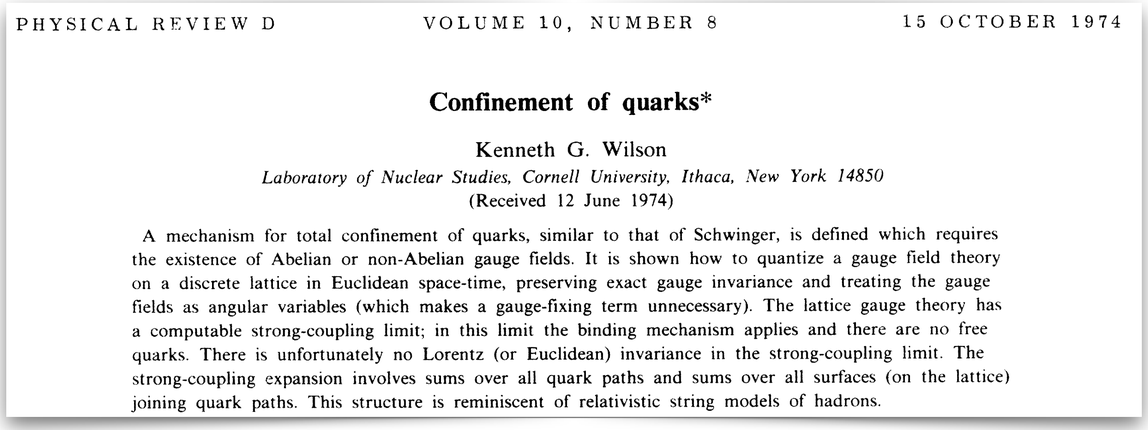

PHYSICAL REVIEW D VOLUME 10, NUMBER 8 15 OCTOBER 1974

Confinement of quarks*

Kenneth G. Wilson
Laboratory of Nuclear Studies, Cornell University, Ithaca, New York 14850
(Received 12 June 1974)

A mechanism for total confinement of quarks, similar to that of Schwinger, is defined which requires the existence of Abelian or non-Abelian gauge fields. It is shown how to quantize a gauge field theory on a discrete lattice in Euclidean space-time, preserving exact gauge invariance and treating the gauge fields as angular variables (which makes a gauge-fixing term unnecessary). The lattice gauge theory has a computable strong-coupling limit; in this limit the binding mechanism applies and there are no free quarks. There is unfortunately no Lorentz (or Euclidean) invariance in the strong-coupling limit. The strong-coupling expansion involves sums over all quark paths and sums over all surfaces (on the lattice) joining quark paths. This structure is reminiscent of relativistic string models of hadrons.

While this work only provided a plausible argument for quark confinement, it also introduced lattice gauge theory, which has since become an invaluable tool for studying the low-energy behavior of QCD.

- This paper also draws on the path integral formulation of quantum mechanics and quantum field theory, introduced by Richard Feynman.

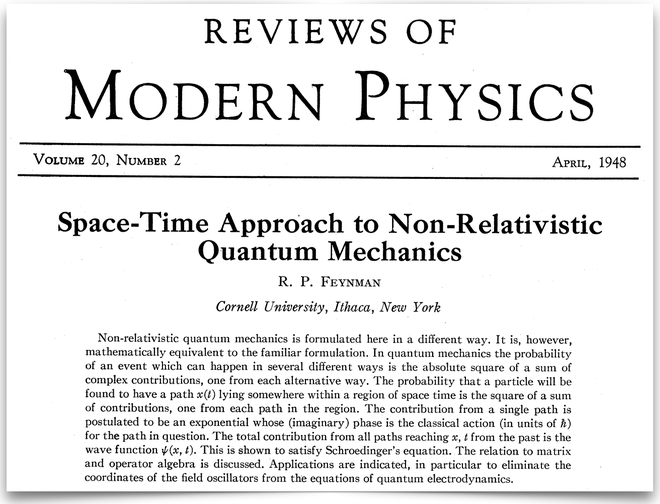

REVIEWS OF
MODERN PHYSICS

VOLUME 20, NUMBER 2 APRIL, 1948

Space-Time Approach to Non-Relativistic Quantum Mechanics

R. P. FEYNMAN
Cornell University, Ithaca, New York

Non-relativistic quantum mechanics is formulated here in a different way. It is, however, mathematically equivalent to the familiar formulation. In quantum mechanics the probability of an event which can happen in several different ways is the absolute square of a sum of complex contributions, one from each alternative way. The probability that a particle will be found to have a path $x(t)$ lying somewhere within a region of space time is the square of a sum of contributions, one from each path in the region. The contribution from a single path is postulated to be an exponential whose (imaginary) phase is the classical action (in units of $\hbar$) for the path in question. The total contribution from all paths reaching x, t from the past is the wave function $\psi(x, t)$. This is shown to satisfy Schroedinger's equation. The relation to matrix and operator algebra is discussed. Applications are indicated, in particular to eliminate the coordinates of the field oscillators from the equations of quantum electrodynamics.

- 1979, Michael Creutz first numerical simulation of a non Abelian gauge theory.

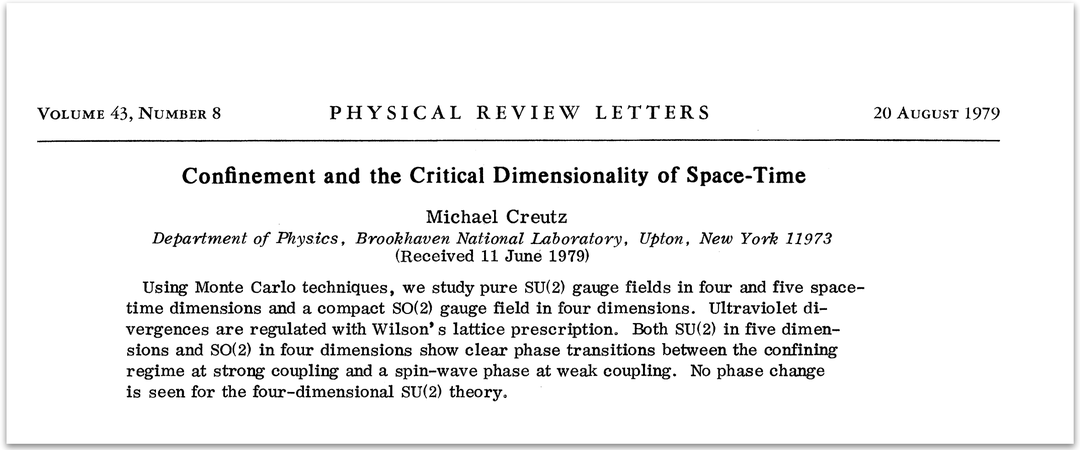

VOLUME 43, NUMBER 8 PHYSICAL REVIEW LETTERS 20 AUGUST 1979

Confinement and the Critical Dimensionality of Space-Time

Michael Creutz
Department of Physics, Brookhaven National Laboratory, Upton, New York 11973
(Received 11 June 1979)

Using Monte Carlo techniques, we study pure SU(2) gauge fields in four and five space-time dimensions and a compact SO(2) gauge field in four dimensions. Ultraviolet divergences are regulated with Wilson's lattice prescription. Both SU(2) in five dimensions and SO(2) in four dimensions show clear phase transitions between the confining regime at strong coupling and a spin-wave phase at weak coupling. No phase change is seen for the four-dimensional SU(2) theory.

Confinement of quarks and QCD on spacetime lattices (cont'd)

- During the early development of lattice QCD, the Hamiltonian formulation of lattice gauge theory was also proposed by Kogut and Susskind.

PHYSICAL REVIEW D VOLUME 11, NUMBER 2 15 JANUARY 1975

Hamiltonian formulation of Wilson's lattice gauge theories

John Kogut*
Laboratory of Nuclear Studies, Cornell University, Ithaca, New York 14853

Leonard Susskind†
Belfer Graduate School of Science, Yeshiva University, New York, New York
and Tel Aviv University, Ramat Aviv, Israel
and Laboratory of Nuclear Studies, Cornell University, Ithaca, New York

(Received 9 July 1974)

Wilson's lattice gauge model is presented as a canonical Hamiltonian theory. The structure of the model is reduced to the interactions of an infinite collection of coupled rigid rotators. The gauge-invariant configuration space consists of a collection of strings with quarks at their ends. The strings are lines of non-Abelian electric flux. In the strong-coupling limit the dynamics is best described in terms of these strings. Quark confinement is a result of the inability to break a string without producing a pair.

- R.P. Feynman: early ideas for simulating physical systems using quantum computers.

International Journal of Theoretical Physics, Vol. 21, Nos. 6/7, 1982

Simulating Physics with Computers

Richard P. Feynman

Department of Physics, California Institute of Technology, Pasadena, California 91107

Received May 7, 1981

4. QUANTUM COMPUTERS—UNIVERSAL QUANTUM SIMULATORS

- More recently, this Hamiltonian approach has opened up the exciting possibility of simulating QCD on a quantum computer.

Simulating quantum field theory with a quantum computer

John Preskill*
Institute for Quantum Information and Matter
Walter Burke Institute for Theoretical Physics
California Institute of Technology, Pasadena CA 91125, USA
E-mail: preskill@caltech.edu

Forthcoming exascale digital computers will further advance our knowledge of quantum chromodynamics, but formidable challenges will remain. In particular, Euclidean Monte Carlo methods are not well suited for studying real-time evolution in hadronic collisions, or the properties of hadronic matter at nonzero temperature and chemical potential. Digital computers may never be able to achieve accurate simulations of such phenomena in QCD and other strongly-coupled field theories; quantum computers will do so eventually, though I'm not sure when. Progress toward quantum simulation of quantum field theory will require the collaborative efforts of quantumists and field theorists, and though the physics payoff may still be far away, it's worthwhile to get started now. Today's research can hasten the arrival of a new era in which quantum simulation fuels rapid progress in fundamental physics.

The 36th Annual International Symposium on Lattice Field Theory - LATTICE2018
22-28 July, 2018
Michigan State University, East Lansing, Michigan, USA.

LATTICE QCD

(Quantum Chromo Dynamics on a discrete space-time lattice)

Ken Wilson (1974) —> space-time discretisation —> lattice regularization of QCD —>

nonperturbative calculations by numerical evaluation of the Feynman path integral that defines the theory

$$\langle \mathcal{O}(U,q,\bar{q})\rangle = (1/Z)\int [dU]\prod_f [dq_f][d\bar{q}_f]\mathcal{O}(U,q,\bar{q})e^{-S_g[U]-\sum_f \bar{q}_f(D[U]+m_f)q_f}$$

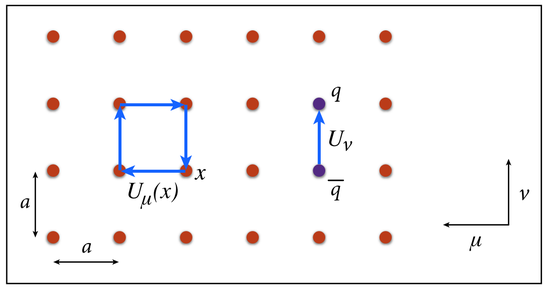

$$Z = \int [dU] e^{-S_g[U]} \prod_f \det(D[U]+m_f)$$

hyper cubic lattice

$$V_{\rm lat} = N_s^3 \times N_t$$

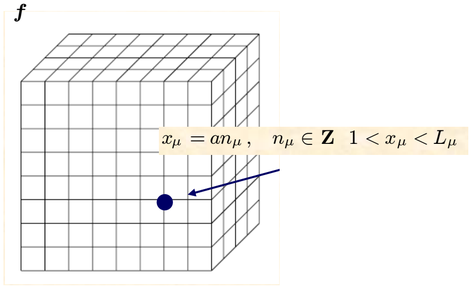

Equivalence with Classical Statistical Mechanics

Quantum Field Theory in d space-time dimensions ⟷ **Classical Statistical Mechanics in d spatial dimensions**

In principle, to take the true continuum limit:

- Thermodynamic limit:

$$\mathbf{N_s \to \infty\ ,\ N_t \to \infty}$$

- Continuum limit:

$$\mathbf{a(\beta) \to 0} \quad \Leftrightarrow \quad \beta \equiv \frac{6}{g^2} \to \infty$$

However, this is not feasible in a numerical calculation. The practical recipe is:

- Compute physical observables for a few values of the lattice spacing $\mathbf{a}(\beta)$.
- Choose $\mathbf{N_s}$ and $\mathbf{N_t}$ in order that the physical extension of the lattice box $\mathbf{a^3 N_s^3 \times a N_t}$ remains fixed for the different values of $\mathbf{a}(\beta)$.
- Study (*scaling analysis*) the dependence from $\mathbf{a}(\beta)$ of the results at fixed physical volume and extrapolate the results to $\mathbf{a}(\beta) \to \mathbf{0}$.
  The extrapolation to $\mathbf{a}(\beta) \to \mathbf{0}$ can then be repeated for different physical sizes of the lattice box and this allows also to extrapolate the data to infinite physical volume.

The Lattice QCD workflow

Numerical evaluation (using Monte Carlo methods) of the functional integral for the operators corresponding to specific physical observables

GENERATION (Monte Carlo sampling phase)

- Gauge-field configurations U, distributed according to the QCD action, are generated by means of Monte Carlo techniques
- A certain number of configurations (each consisting of a fixed number of complex numbers) are stored on disk for subsequent analysis.

$$P_{\mathrm{eq}}(U) = \frac{1}{\mathcal{Z}}\mathrm{Det}(M^{\dagger}M)e^{-S(U)}$$

MEASUREMENT

- Measurements of physical observables are performed on the stored gauge configurations.

$$\mathcal{O}(U)$$

ANALYSIS

- Averaging of the measurements over configurations, extrapolations to certain limits.
- Possible comparison of the outcome of these calculations with experimental results.

$$\langle \mathcal{O} \rangle \approx \overline{\mathcal{O}} = \frac{1}{N}\sum_{U} \mathcal{O}(U)$$

highly computing demanding tasks !

Parallel to the development of Lattice Quantum Chromo Dynamics (LQCD), there have been equally remarkable advances in computer design and implementation.

It soon became clear that parallel assemblies of computing nodes offered the most effective route to the highest computational performance.

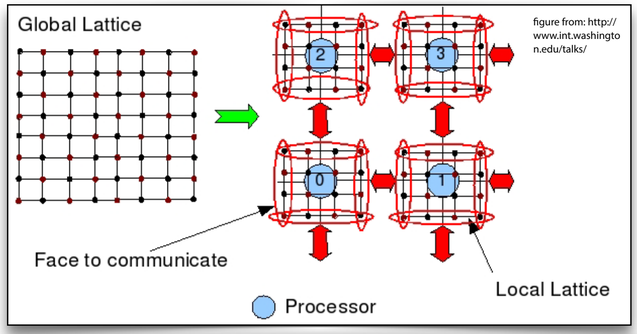

ideal case of the parallel computation paradigm !

Space-time lattice

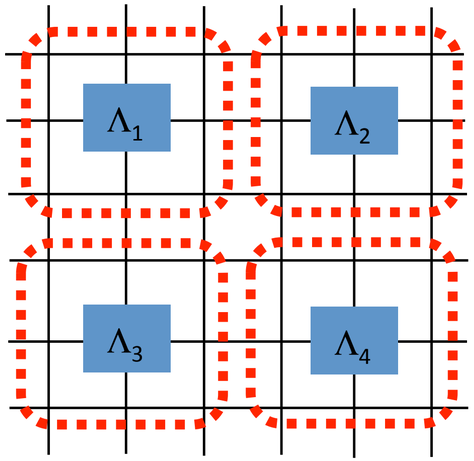

Data for a single lattice site or block of sites may be stored in the local memory of each processor and the four-dimensional lattice mapped down to the network of the machine. Generally this can be done so that only nearest-neighbour data communication is required in the generation of gauge field configurations.

Processor array

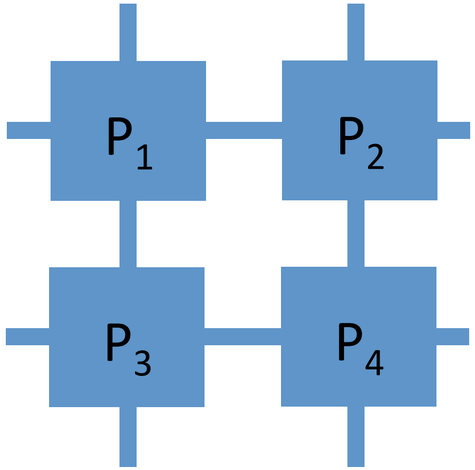

Locality: *(property of the field theoretic description of fundamental interactions)*

- the numerical operations at a site n can be carried out independently of those at a site m unless the pair is within the limited neighborhood of each other;
- calculations by a given processor can be carried out independently of those by the other processors, except that the processors with overlapping boundaries have to exchange values of fields in the boundaries before and/or after the calculations in each sub lattice;
- for a fixed lattice size, the computation time can be reduced by a factor N_P , and for a fixed sub-lattice size, one can enlarge the total lattice size proportionately to the number of processors N_P without increasing the computation time.

Lattice QCD and parallel computers building

LQCD collaborations have also played a crucial role in the development of specialized hardware. The architecture of modern supercomputers, like the renowned IBM Blue Gene/Q, was influenced by the design of computers specifically tailored for lattice QCD simulations.

name	year	authors	peak speed
Columbia	1984	Christ-Terrano	–
Columbia-16	1985	Christ et al	0.25 GFlop/s
APE1	**1988**	**Cabibbo-Parisi**	**1 GFlop/s**
Columbia-64	1987	Christ et al	1 GFlop/s
Columbia-256	1989	Christ et al	16 GFlop/s
ACPMAPS	1991	Mackenzie et al	5 GFlop/s
QCDPAX	1991	Iwasaki-Hoshino	14 GFlop/s
GF11	1992	Weingarten	11 GFlop/s
APE100	**1994**	**APE Collab.**	**0.1 TFlop/s**
CP-PACS	1996	Iwasaki et al	0.6 TFlop/s
QCDSP	1998	Christ et al	0.6 TFlop/s
APEmille	**2000**	**APE Collab.**	**0.8 TFlop/s**
apeNEXT	**2004**	**APE Collab.**	**10 TFlop/s**
QCDOC	2005	Christ et al	10 TFlop/s
PACS-CS	2006	Ukawa et al	14 TFlop/s
QCDCQ	2011	Christ et al	500 TFlop/s
QPACE	2012	Wettig et al	200 TFlop/s

APE100

APEmille

MAY 2024

TOP 500 The List.

top500.org

			SITE	COUNTRY	CORES	RMAX PFLOP/S	POWER MW
1	**Frontier**	HPE Cray EX235a, AMD Opt 3rd Gen EPYC (64C 2GHz), AMD Instinct MI250X, Slingshot-11	DOE/SC/ORNL	USA	8,699,904	1,206.0	22.7
2	**Aurora**	HPE Cray EX - Intel Exascale Compute Blade, Xeon CPU Max 9470 (52C 2.4GHz), Intel Data Center GPU Max, Slingshot-11	DOE/SC/ANL	USA	9,264,128	1,012.0	38.7
3	**Eagle**	Microsoft NDv5, Xeon Platinum 8480C (48C 2GHz), NVIDIA H100, NVIDIA Infiniband NDR	Microsoft Azure	USA	1,123,200	561.2	
4	**Fugaku**	Fujitsu A64FX (48C, 2.2GHz), Tofu Interconnect D	RIKEN R-CCS	Japan	7,630,848	442.0	29.9
5	**LUMI**	HPE Cray EX235a, AMD Opt 3rd Gen EPYC (64C 2GHz), AMD Instinct MI250X, Slingshot-11	EuroHPC/CSC	Finland	2,220,288	379.7	6.01

PERFORMANCE DEVELOPMENT

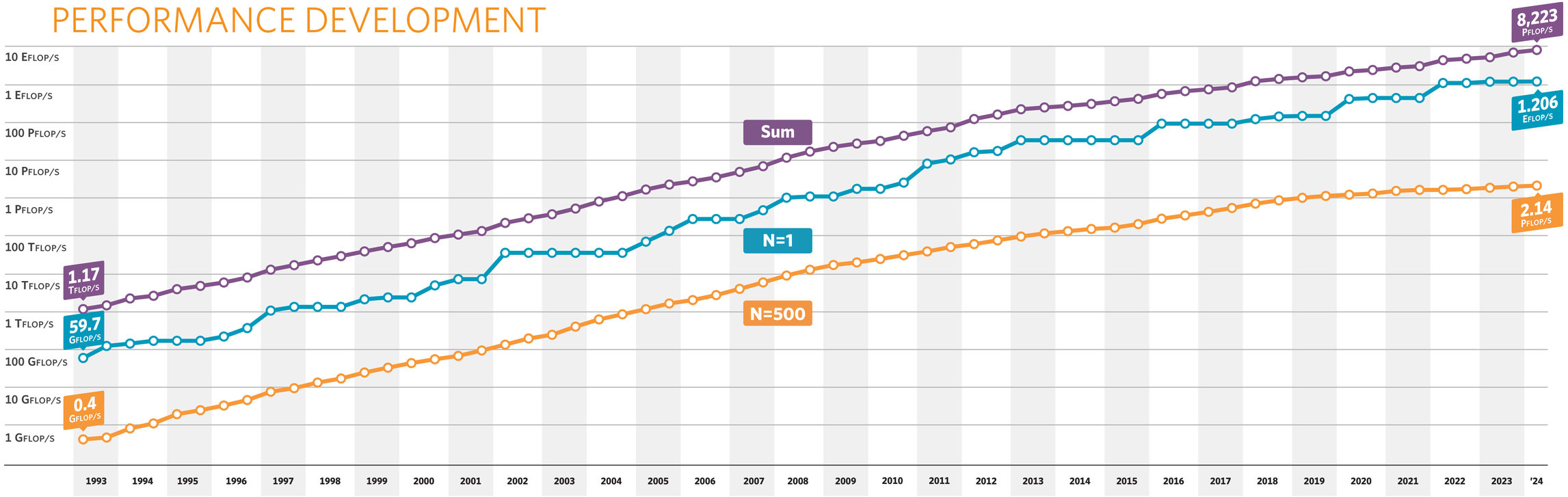

Main computing resources in Europe

https://eurohpc-ju.europa.eu/supercomputers/our-supercomputers_en

EuroHPC Joint Undertaking

LUMI supercomputer
375 PFlop/s - FINLAND

- LUMI-G (accelerated partition)
  2978 nodes with 4 AMD MI250x GPUs and a single 64 cores AMD EPYC "Trento" CPU.
  379.70 PFlop/s HPL
- LUMI-C (CPU partition)
  2048 CPU-based compute nodes (128 cores/node AMD EPYC)

LEONARDO supercomputer
250 PFlop/s - ITALY

- LEONARDO-booster 3456 nodes
  1 x CPU Intel Xeon 8358 32 cores, 2,6 GHz
  512 (8 x 64) GB RAM DDR4 3200 MHz
  4 X Nvidia custom Ampere GPU 64GB HBM2
  2 x NVidia HDR 2×100 Gb/s cards
- LEONARDO-GP 1536 nodes
  2x Intel Sapphire Rapids, 56 cores, 4.8 GHz
  512 (16 x 32) GB RAM DDR5 4800 MHz
  3xNvidia HDR cards 1x100Gb/s cards
  8 TB NVM

LISA-GPU (> 100 PFlops HPL)
LISA-CPU (> 6 PFlops HPL)

MARENOSTRUM 5
275 PFlop/s - SPAIN

- MareNostrum 5 ACC (Accelerated Partition)
  1120 nodes based in Intel Sapphire rapids (64 cores/node) and Nvidia Hopper GPUs (4 GPUs/node). 230 PFlops HPL
- MareNostrum 5 GPP (General Purpose Partition)
  6408 nodes based in Intel Sapphire rapids (112 cores/ node). 45 PFlops HPL

Main computing resources in Europe (cont'd)

MELUXINA supercomputer
12.81 PFlop/s - LUXEMBOURG

KAROLINA supercomputer
9.59 PFlop/s - CZECH Republic

DEUCALION supercomputer
7.22 PFlop/s - PORTUGAL

HPC Vega IZUM
6.92 PFlop/s - SLOVENIA

DISCOVERER supercomputer
4.51 PFlop/s - BULGARIA

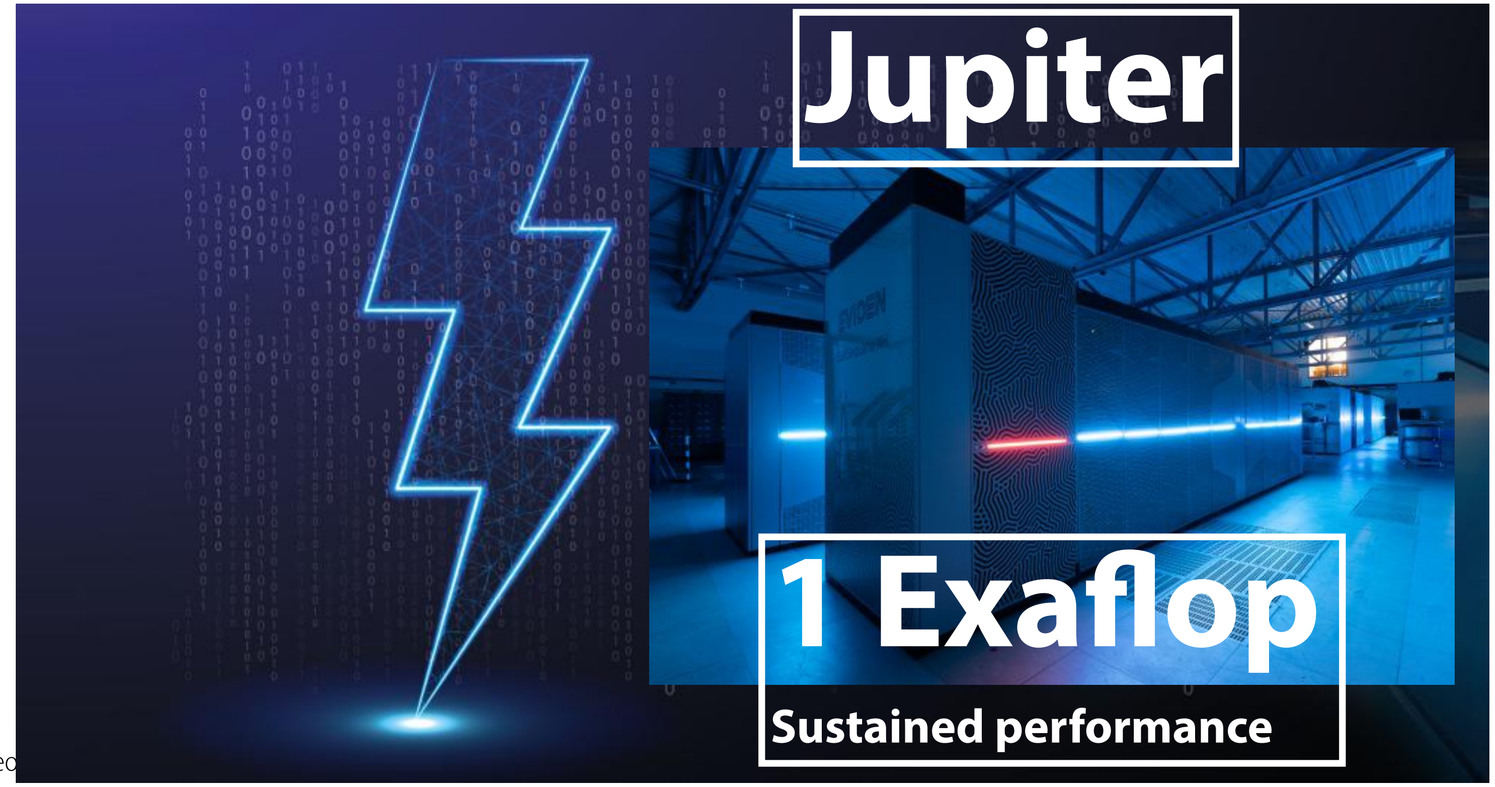

will be the first EuroHPC exascale(*) supercomputer (@Julich-Germany)

(*) 10^{18} Flop/s

Example of
Lattice QCD computation @ Exascale Frontier

Physics goals:

calculations with ensembles of gauge fields with physical volumes V large enough to ensure that finite-volume effects are under control.

Simulation with up/down, strange, charm and bottom quarks at their physical masses with physical volume $\mathbf{V = (10\ fm)^4}$ at a lattice spacing $\mathbf{a = 0.04}$ fm ($\mathbf{a^{-1} \sim 5}$ GeV) (lattice size $\mathbf{256^3 \times 512}$)

- **Lattice volume: $\mathbf{V = 256^3 \times 512}$ —> $\mathbf{4V}$ SU(3) matrices —> $\mathbf{4V \times 18}$ real numbers —> $\mathbf{\sim 2.5}$ TB storage per lattice configuration (with a local volume of 8^4 —> 2.1×10^6 cores**

- $\mathbf{\sim 12,000}$ Exaflop hours $= \mathbf{12,000 \times (3600 \times 10^{18})}$ floating-point operations

Lattice QCD

Study of QCD in extreme conditions

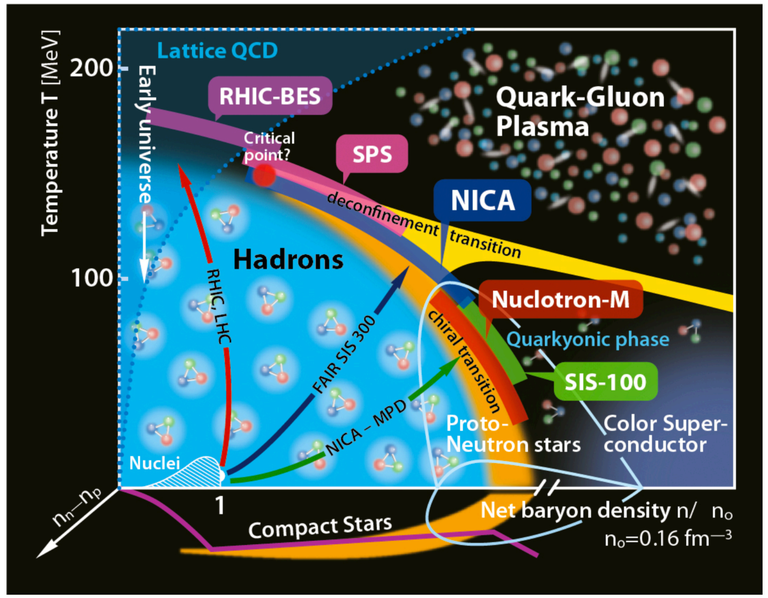

Precision studies of flavor physics, within and beyond the Standard Model

The latest lattice QCD results related to the **muon g-2 problem** have significantly reduced the discrepancy between theoretical predictions and experimental measurements. The new calculations now differ from the experimental measurements **by only 0.9 standard deviations**.

This finding is critical as it challenges the previously observed tension between experiment and theory, which had fueled speculation about new physics beyond the Standard Model.

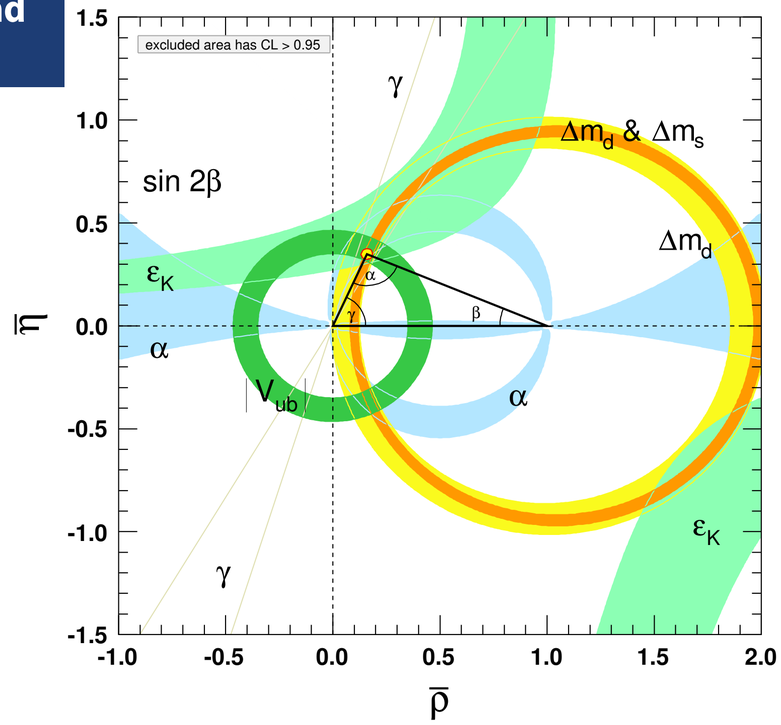

- Lattice QCD is an essential tool for obtaining precise first-principle theoretical predictions of the hadronic processes underlying many key experimental searches.
- As experimental measurements become more precise, lattice QCD will play an increasingly important role in providing the necessary matching theoretical precision.
- Achieving the needed precision requires simulations on lattices with significantly increased resolution.

A large number of computing nodes is required (up to $\mathcal{O}(10^5)$ cores. On the largest scales the challenge lies in efficiently and effectively exchanging data among the processors or nodes —> MPI, MPI+OpenMP.

The **development of numerical algorithms** is crucial: over the history of lattice gauge theory calculations, the improvement from algorithm development has been similar to the gain from Moore's law.

THE COLOR CONFINEMENT

- Color confinement is supported by a wide range of experimental observations: in high-energy particle collisions, quarks and gluons are never observed as free particles but always emerge as part of bound states (hadrons).

- Understanding color confinement is crucial for explaining why quarks and gluons are never observed as free particles but are always confined within hadrons.

- While confinement is well-supported by lattice QCD and experimental evidence, providing an analytic proof from first principles remains an open challenge in theoretical physics.

Color confinement is still an unsolved problem

https://www.claymath.org/millennium-problems/

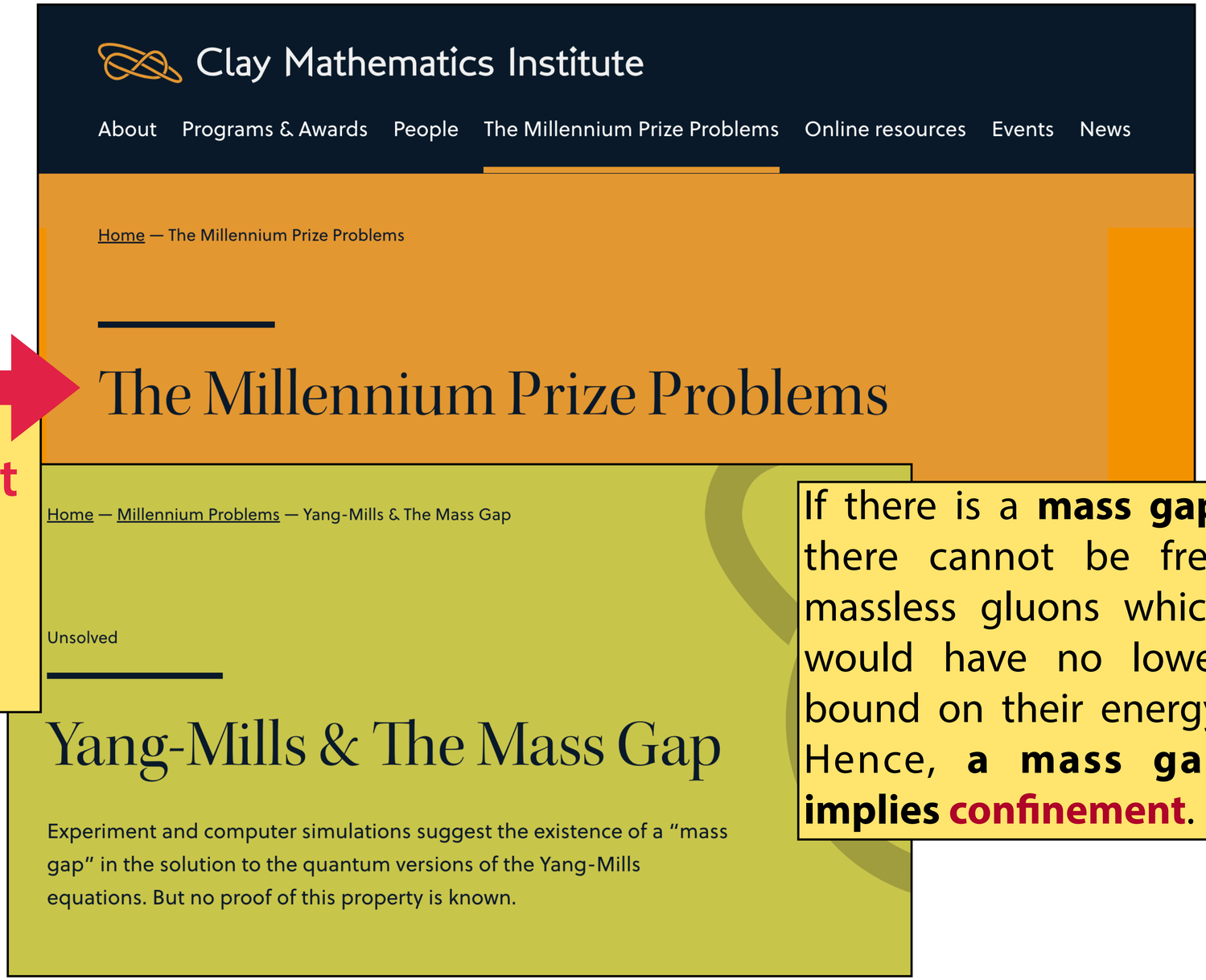

If there is a **mass gap**, there cannot be free massless gluons which would have no lower bound on their energy. Hence, **a mass gap implies confinement**.

THE COLOR CONFINEMENT (cont'd)

- Achieving a detailed understanding of color confinement remains a central goal for nonperturbative studies of QCD and is strictly related to the phase diagram of QCD.

- Lattice numerical simulations have long revealed the emergence of tube-like structures when analyzing the chromoelectric fields between static quarks.

- The observation of these tube-like structures in lattice simulations is related to the linear potential between static color charges and provides direct numerical evidence for color confinement.

- From the phenomenological point of view, the knowledge of the flux tube structures in QCD could provide useful hints to the description of hadronization processes in the Lund string model.

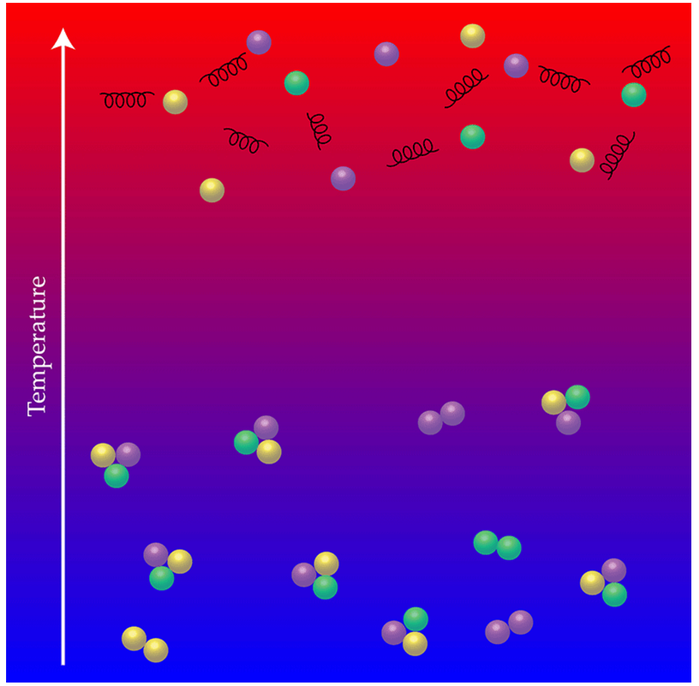

Heavy quark potential – free energy of a static quark-antiquark configuration separated by a distance d.

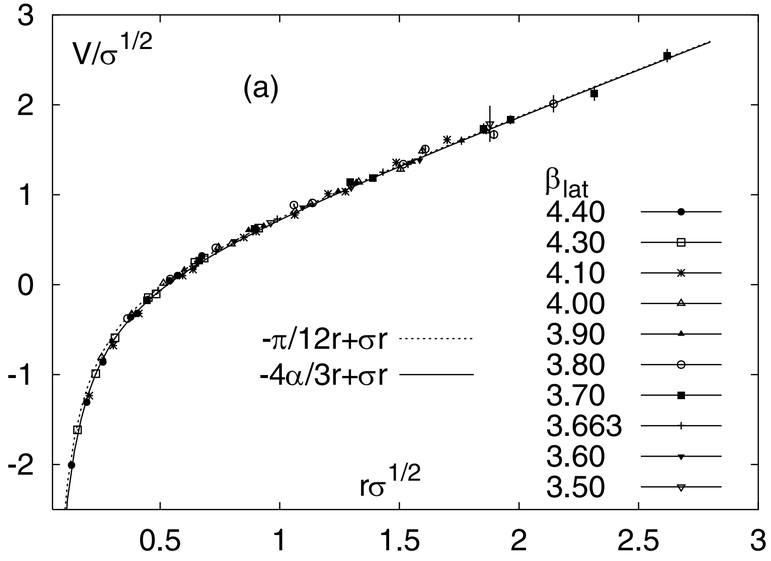

O. Kaczmarek and F. Zantow, [arXiv:hep-lat/0503017].

$$V(d) = -\frac{\pi}{12}\frac{1}{d} + \sigma d$$

σ : string tension

How to measure the chromoelectromagnetic field tensor on the lattice?

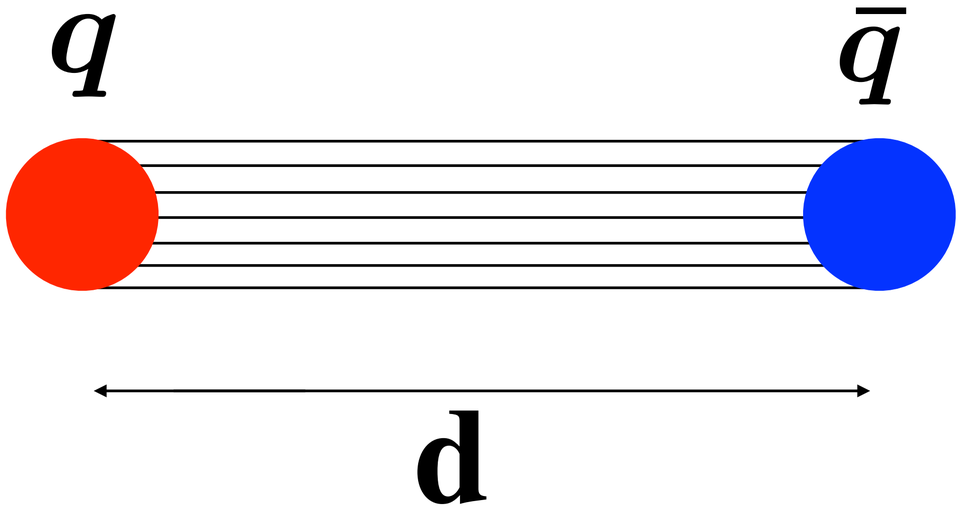

To explore on the lattice the field configurations produced by a static quark-antiquark pair —> connected correlation function (*)

(*) Di Giacomo, Maggiore, Oleínik , NPB347(1990)441

Skala, Faber, Zach, NPB494(1997)293

Kuzmenko, Simonov, PLB494(2000)81

Di Giacomo, Dosch, Shevchenko, Simonov, Phys.Rept.372(2002)319

THE SPATIAL DISTRIBUTION OF THE COLOR FIELDS

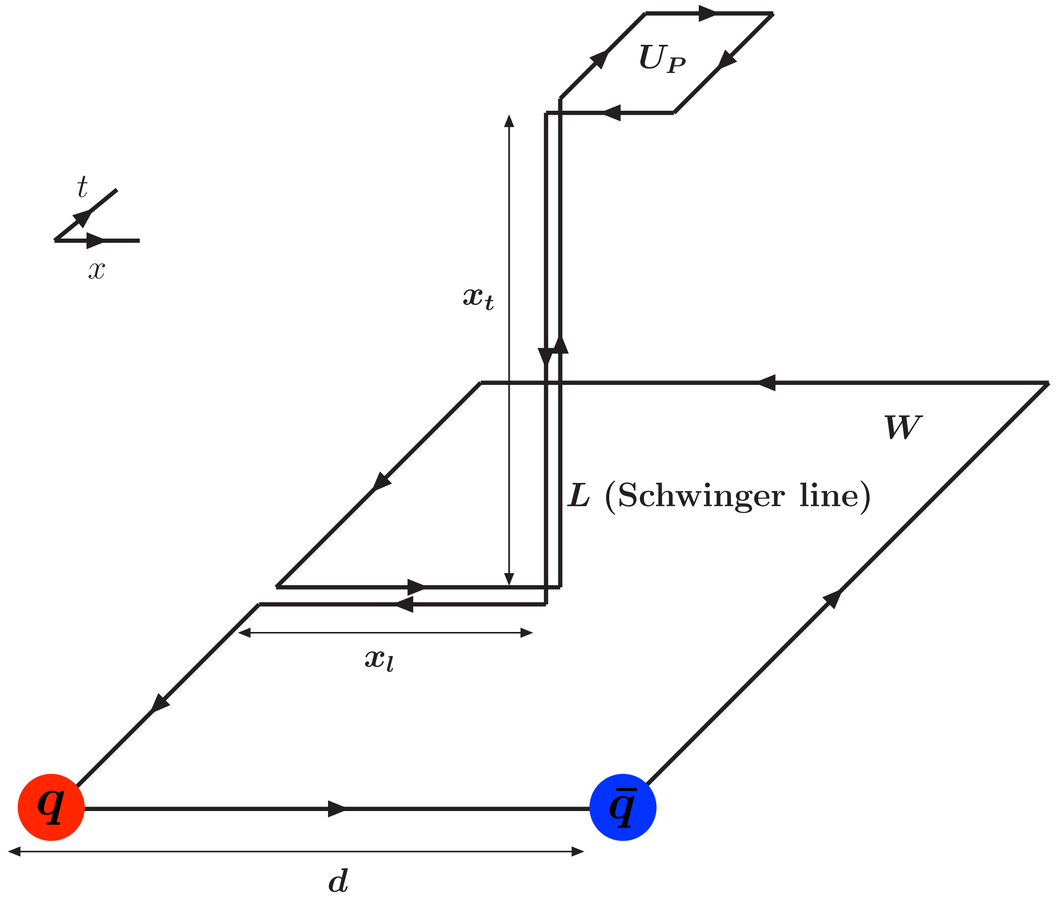

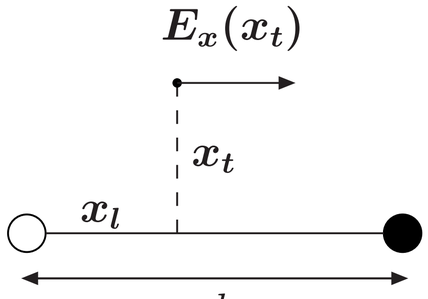

- **lattice measurements of the connected correlation function**

$$\rho^{\text{conn}}_{\mathbf{W},\mu\nu} = \frac{\langle \text{tr}(\mathbf{W}\mathbf{L}\mathbf{U}_\mathbf{P}\mathbf{L}^\dagger)\rangle}{\langle \text{tr}(\mathbf{W})\rangle} - \frac{\mathbf{1}}{\mathbf{N}}\frac{\langle \text{tr}(\mathbf{U}_\mathbf{P})\text{tr}(\mathbf{W})\rangle}{\langle \text{tr}(\mathbf{W})\rangle}$$

- lattice definition of the **gauge-invariant field strength tensor**

$$\rho^{\text{conn}}_{\mathbf{W},\mu\nu} \equiv \mathbf{a^2 g}\langle \mathbf{F}_{\mu\nu}\rangle_{\mathbf{q\bar{q}}} \equiv \mathbf{a^2 g}\ \mathbf{F}_{\mu\nu}$$

- rotating the plaquette relative to the plane of the Wilson loop allows us to extract the **components of the field tensor:**
  - plaquette U_P in the plane $(\hat{\mu}=4,\hat{\nu}=1) \longrightarrow E_x$
  - plaquette U_P in the plane $(\hat{\mu}=4,\hat{\nu}=2) \longrightarrow E_y$
  - plaquette U_P in the plane $(\hat{\mu}=4,\hat{\nu}=3) \longrightarrow E_z$
  - plaquette U_P in the plane $(\hat{\mu}=2,\hat{\nu}=3) \longrightarrow B_x$
  - plaquette U_P in the plane $(\hat{\mu}=3,\hat{\nu}=1) \longrightarrow B_y$
  - plaquette U_P in the plane $(\hat{\mu}=4,\hat{\nu}=2) \longrightarrow B_z$

SYMMETRY: The fields take on the same values at spatial points connected by rotations around the axis on which the sources are located

Our earliest investigations

$$\rho^{conn}_{W,\mu\nu} \equiv \quad a^2 g \langle F_{\mu\nu} \rangle_{q\bar{q}} \quad \equiv \quad a^2 g \, F_{\mu\nu}$$

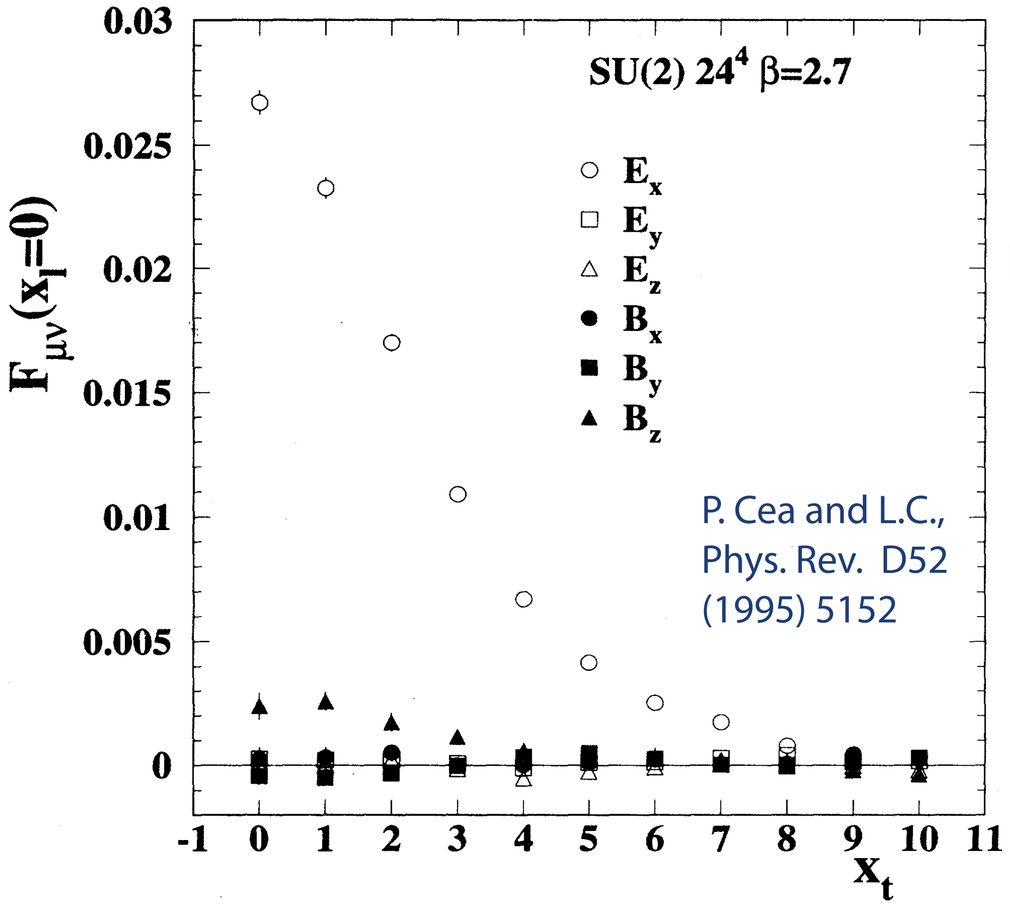

FIG. 2. The field strength tensor $F_{\mu\nu}(x_l, x_t)$ evaluated at $x_l = 0$ on a 24^4 lattice at $\beta = 2.7$, using Wilson loops of size 10×10 in Eq. (2.1).

The flux tube is almost completely formed by the longitudinal chromoelectric field.

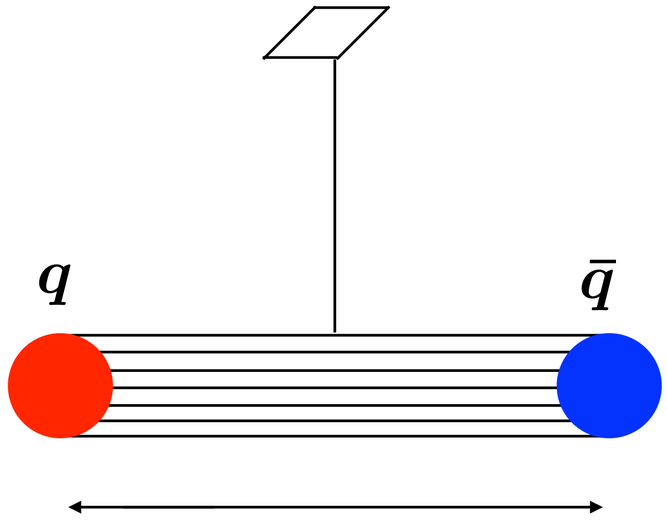

$$d = 10\,a$$

Systematic study of flux tubes in the case of:

- SU(3) pure gauge theory at $T = 0$
- SU(3) pure gauge theory at $T \neq 0$
- QCD with (2+1) flavors at $T = 0$

Ongoing and future studies:

- QCD with (2+1) flavors at $T \neq 0$
- QCD with (2+1) flavors at $T \neq 0$ in presence of background fields (magnetic or chromomagnetic) and/or at finite baryon density

My collaborators

Marshall Baker *(Univ. of Washington, Seattle)*

Paolo Cea *(INFN, Bari)*

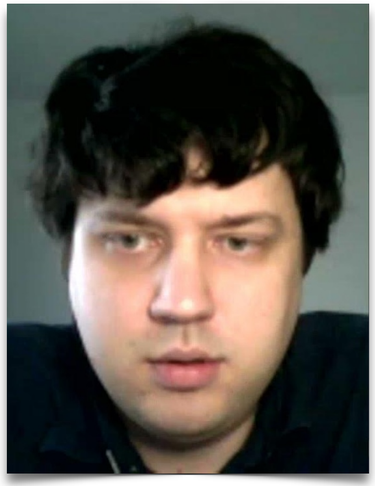

Volodymyr Chelnokov *(Goethe Universität, Frankfurt)*

Francesca Cuteri *(Goethe Universität, Frankfurt)*

Alessandro Papa *(Univ. Calabria and INFN, Cosenza)*

SU(3) T = 0 48^4 lattice $\beta = 6.240$ d = 1.14 fm

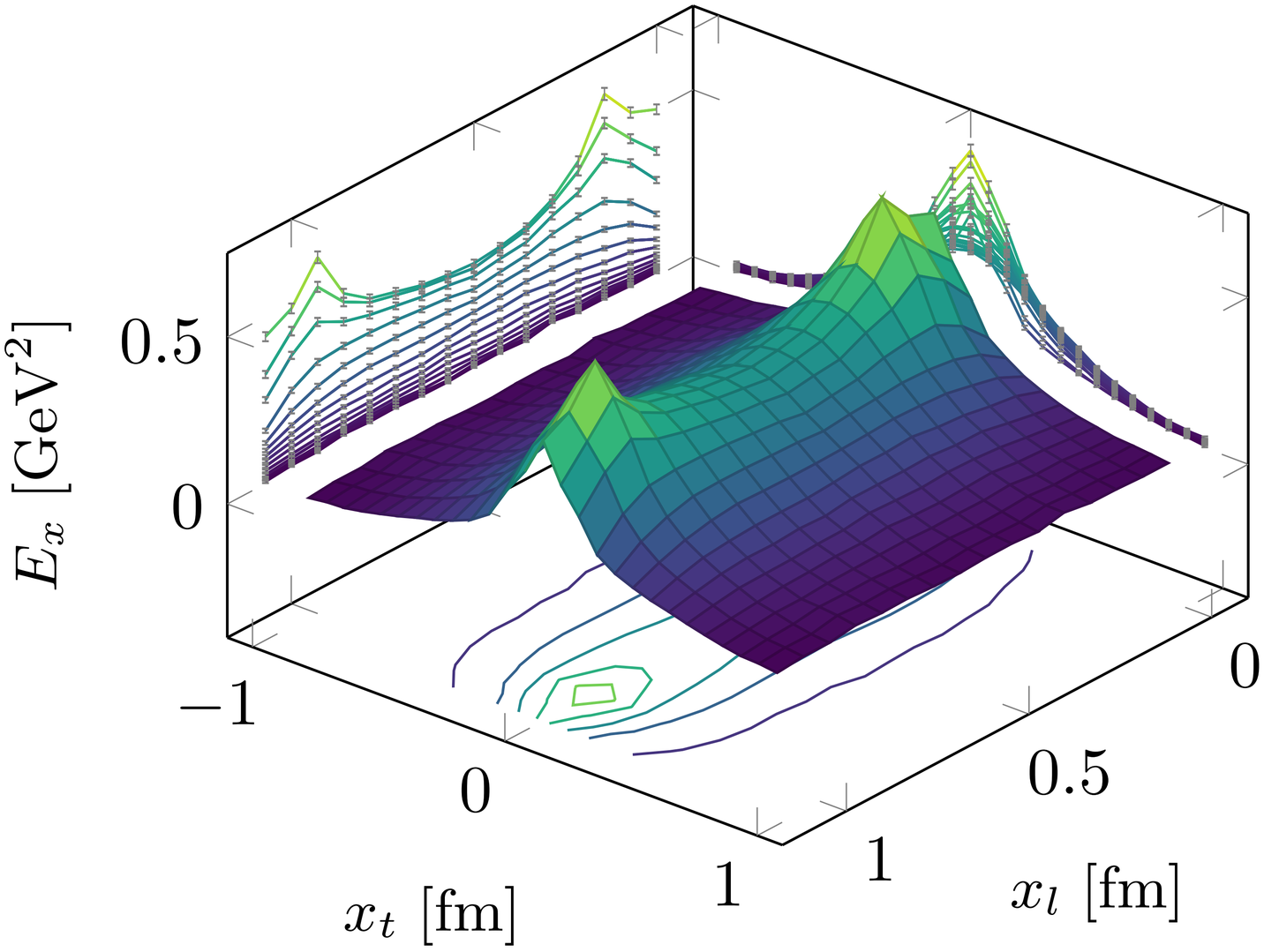

Full profile of the chromoelectric longitudinal field

$E_x(x_t, x_l)$

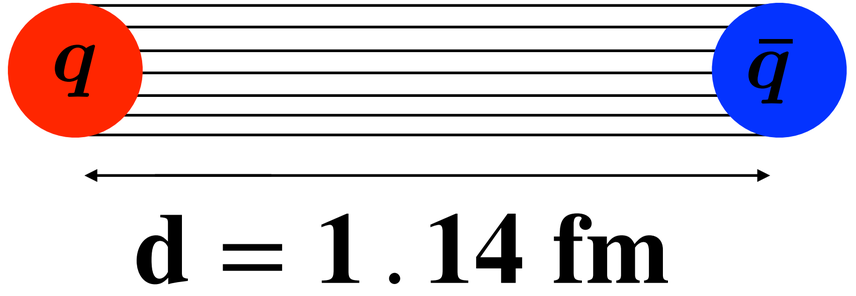

[M. Baker, P. Cea, V. Chelnolov, L.C., F. Cuteri, A. Papa, arXiv:1810.07133, arXiv:1912.04739]

SU(3) T = 0 → The chromoelectromagnetic field tensor

$E_x(x_t, x_l)$

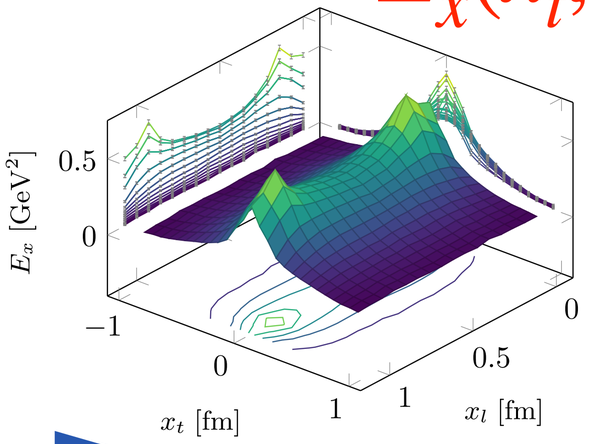

$E_y(x_t, x_l)$

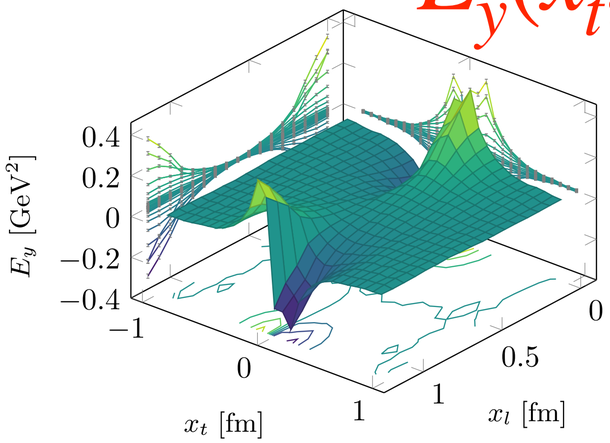

$E_z(x_t, x_l)$

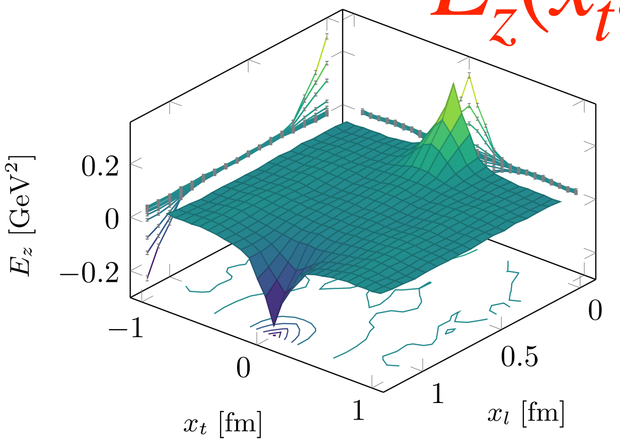

The chromomagnetic field around the sources is compatible with zero within statistical errors.

$B_x(x_t, x_l)$

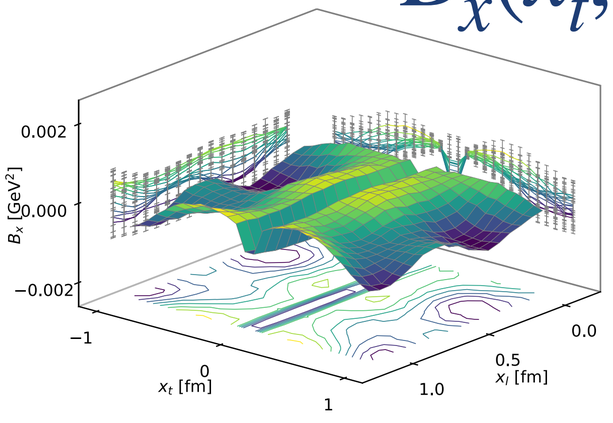

$B_y(x_t, x_l)$

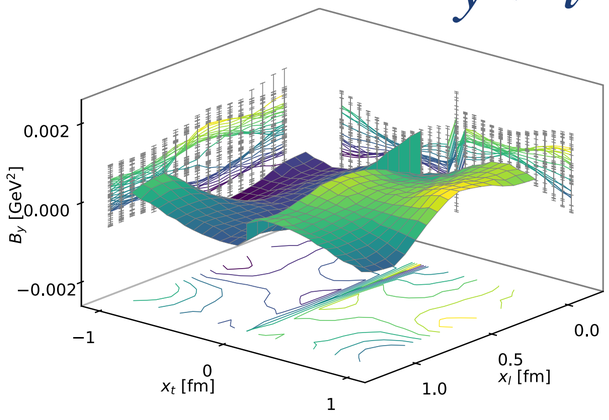

$B_z(x_t, x_l)$

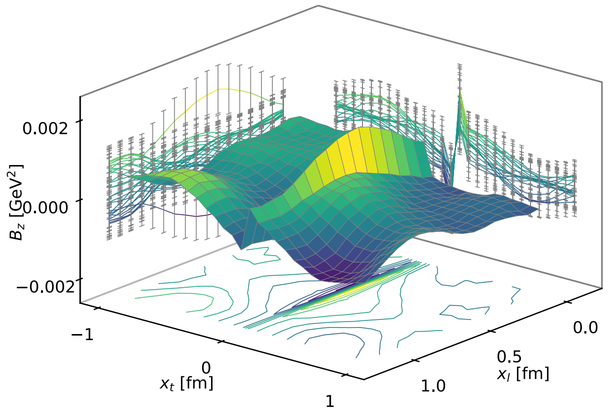

48^4 lattice $\beta = 6.240$ d = 1.14 fm

[M. Baker, P. Cea, V. Chelnolov, L.C., F. Cuteri, A. Papa, arXiv:1810.07133, arXiv:1912.04739]

SU(3)

$\beta = 6.370 \quad d = 0.85$ fm

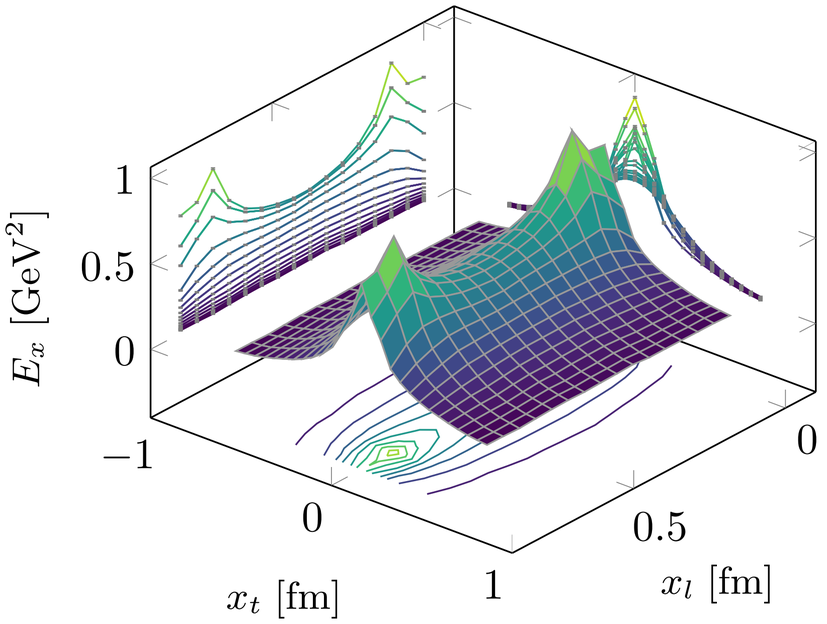

The dominant component of the chromoelectric field is longitudinal.

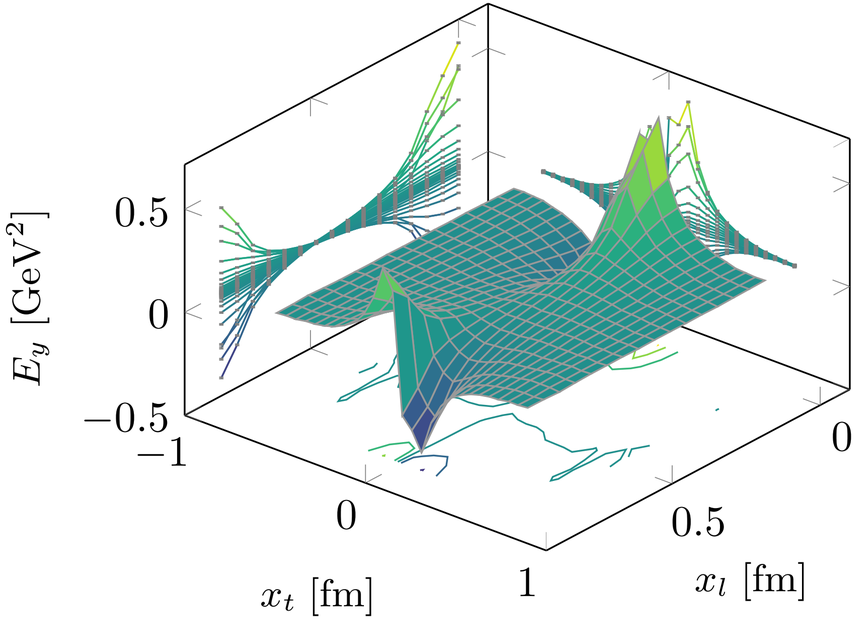

The components of the chromoelectric field transverse to the line connecting the sources can be matched to an effective Coulomb-like field.

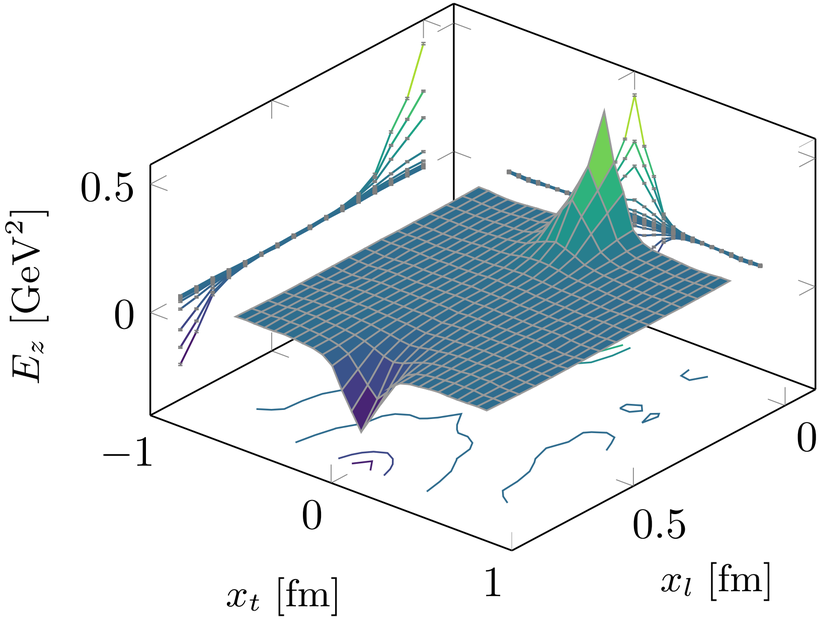

[M. Baker, P. Cea, V. Chelnolov, L.C., F. Cuteri, A. Papa, arXiv:1810.07133, arXiv:1912.04739]

Transverse chromoelectric components: effective Coulomb-like field

The components of the chromoelectric field transverse to the line connecting the sources can be matched to an effective Coulomb-like field $\vec{\mathbf{E}}^{\mathbf{C}}(\vec{\mathbf{r}})$ satisfying the following conditions:

- The transverse component $\mathbf{E_y}$ of the chromoelectric field is identified with the transverse component $\mathbf{E_y^C}$ of the perturbative field:

$$\mathbf{E_y^C} \equiv \mathbf{E_y}$$

- The perturbative field $\mathbf{E^C}$ is irrotational: $\vec{\nabla} \times \vec{\mathbf{E}}^{\mathrm{C}} = \mathbf{0}$

The lattice procedure to evaluate the perturbative Coulomb-like contribution to the longitudinal chromoelectric field

The irrotational condition on a discrete lattice (on a plaquette):

$$E_x^{\mathrm{C}}(x,y) + E_y^{\mathrm{C}}(x+1,y) - E_x^{\mathrm{C}}(x,y+1) - E_y^{\mathrm{C}}(x,y) = 0$$

Solve this equation for E_x^C

$$E_x^{\mathrm{C}}(x,y) = \sum_{y'=y}^{y_{\max}} \left(E_y(x,y') - E_y(x+1,y')\right) + E_x^{\mathrm{C}}(x, y_{\max}+1)$$

We further assume: $E_x^{\mathrm{C}}(x, y_{\max}+1) = 0$

The confining field of the QCD flux tube

SU(3) $\beta = 6.370$ d = 16a = 0.85 fm (*)

The longitudinal $\mathbf{E_x}$ can be separated into the **perturbative**, short-distance part $\mathbf{E_x^C}$ and a **nonperturbative** term $\mathbf{E_x^{NP}}$, encoding the confining information, which is shaped as a **smooth flux tube**.

$$\mathbf{E_x^{NP} = E_x - E_x^C}$$

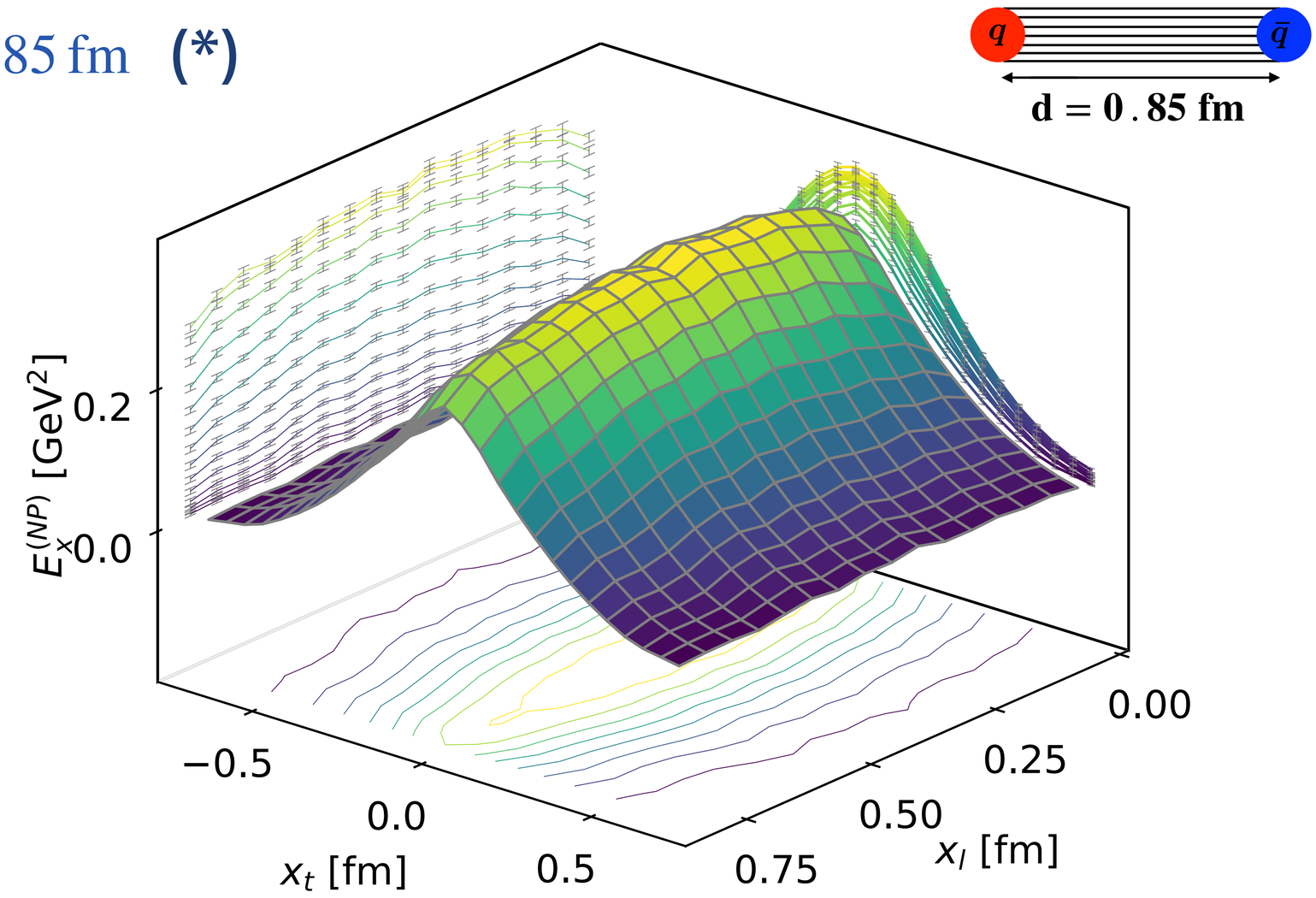

(*) **Lattice scale:**

$a(\beta) = r_0 \times \exp\left[c_0 + c_1(\beta-6) + c_2(\beta-6)^2 + c_3(\beta-6)^3\right]$

$r_0 = 0.5$ fm

$c_0 = -1.6804\,, c_1 = -1.7331$

$c_2 = 0.7849\,, c_3 = -0.4428$

[S. Necco, R. Sommer, arXiv:hep-lat/0108008]

The string tension and the width of the chromoelectric flux tube

We can compute the (square root of the) **string tension** as:

$$\sqrt{\sigma} = \sqrt{\int d^2x_t \frac{(E_x^{\rm NP})^2(x_t)}{2}}$$

This determination can be done:

1) by a direct numerical integration
2) analytically, by fitting the numerical data for the transverse distribution of $E_x^{\rm NP}(x_t)$ to the Clem parameterization of the field surrounding a magnetic vortex in a superconductor:

$$E_x^{\rm NP}(x_t) = \frac{\phi}{2\pi}\frac{\mu^2}{\alpha}\frac{K_0[(\mu^2 x_t^2 + \alpha^2)^{1/2}]}{K_1[\alpha]}$$

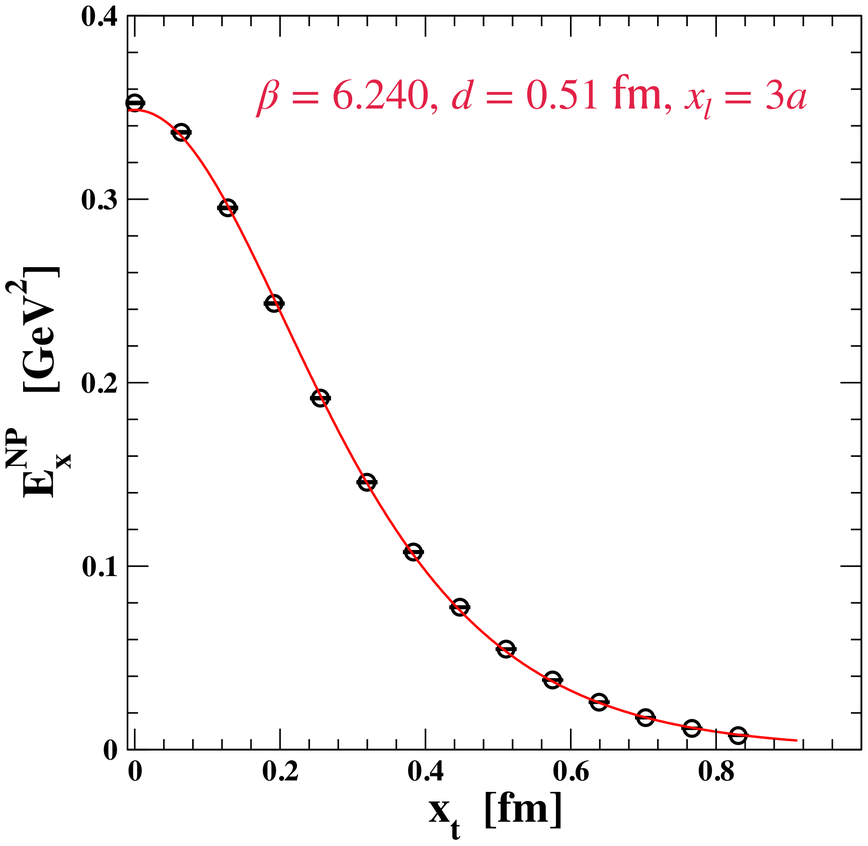

We can compute the **mean square root width of the flux tube**:

$$\sqrt{w^2} = \sqrt{\frac{\int d^2x_t\, x_t^2 E_x(x_t)}{\int d^2x_t\, E_x(x_t)}}$$

SU(3) T = 0

[M. Baker, P. Cea, V. Chelnolov, L.C., F. Cuteri, A. Papa, arXiv:1810.07133, arXiv:1912.04739]

The string tension

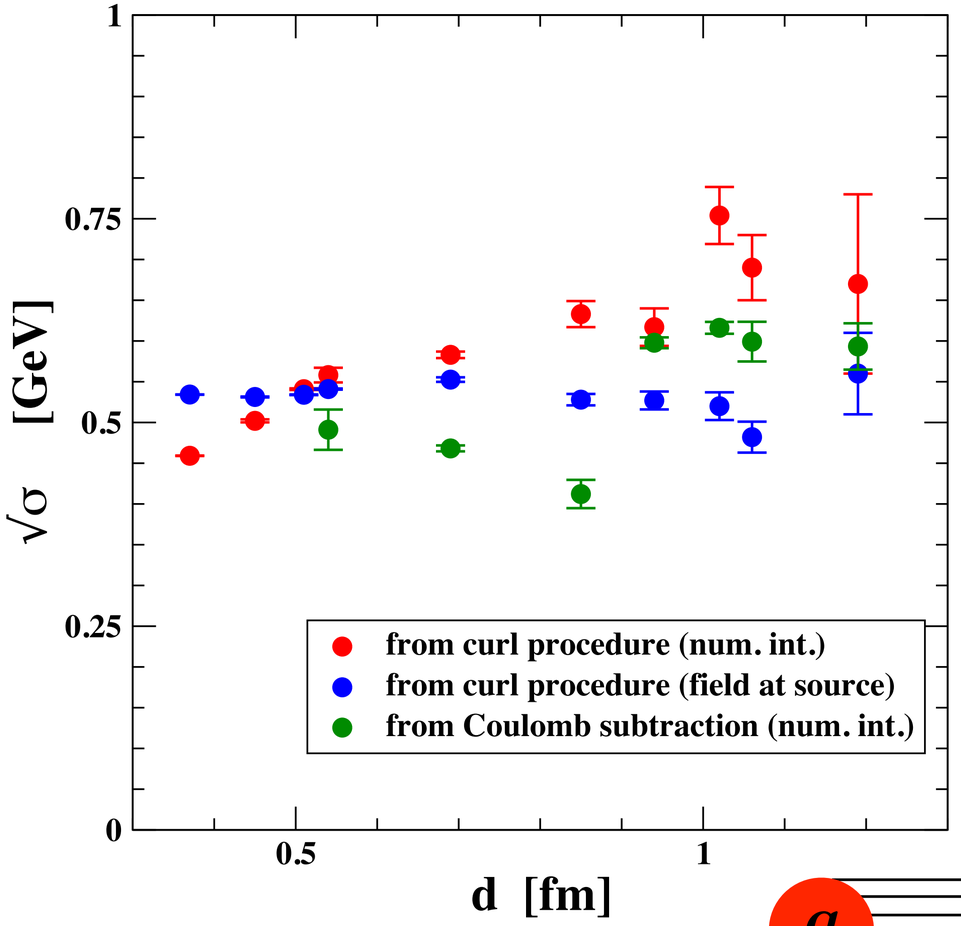

The width of the chromoelectric flux tube

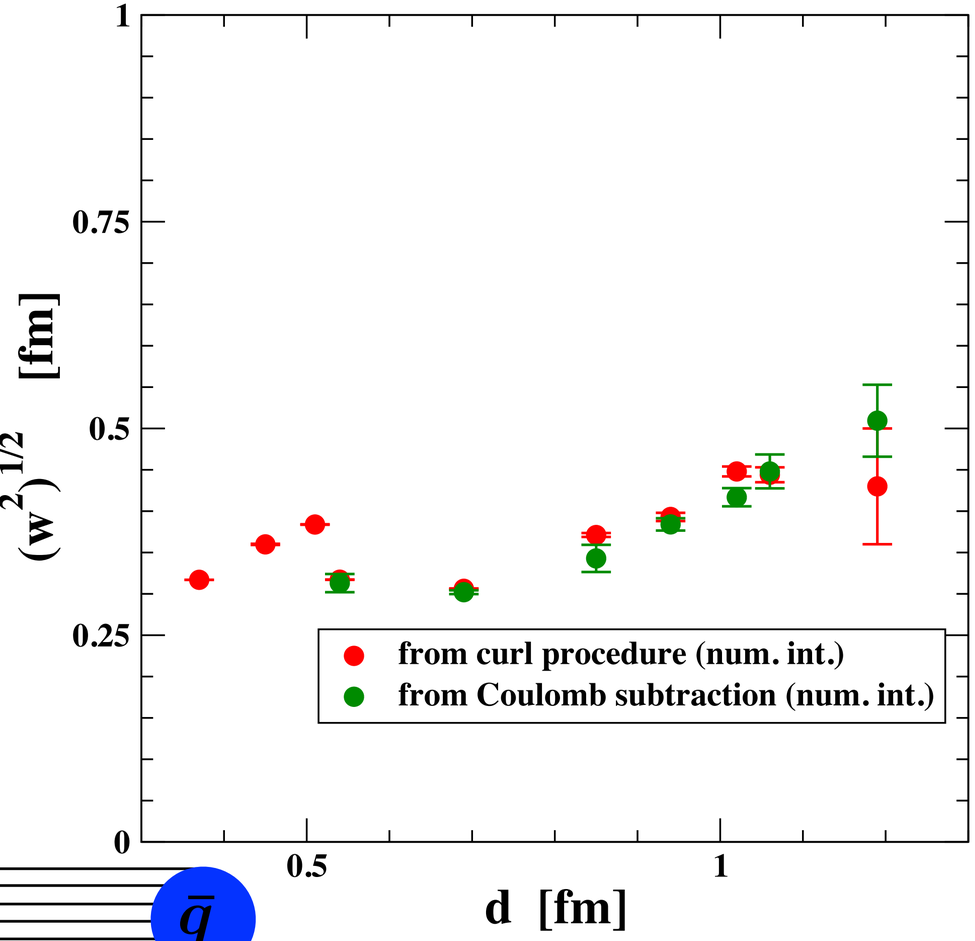

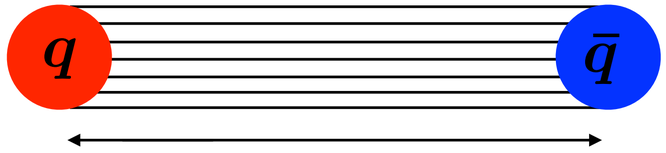

$$0.4\ \text{fm} \leq d \leq 1.2\ \text{fm}$$

SU(3) $T \neq 0$

M. Baker, V. Chelnokov, L. Cosmai, F. Cuteri and A. Papa, [arXiv:2310.04298 [hep-lat]].

Measuring the chromoelectric fields within a flux tube generated by a static quark-antiquark pair in finite-temperature SU(3) gauge theory.

Table 1 Summary of the numerical simulations

Lattice	β	$a(\beta)$ [fm]	d/a	d [fm]	T/T_c	Statistics
$48^3 \times 12$	6.100	0.0789097	12	0.946917	0.8	2400
$48^3 \times 12$	6.381	0.052633	12	0.631597	1.2	340
$48^3 \times 12$	6.381	0.052633	16	0.842129	1.2	1500
$48^3 \times 12$	6.554	0.0420845	15	0.631267	1.5	1100
$32^3 \times 8$	6.248	0.0631757	10	0.631757	1.5	2580
$48^3 \times 12$	6.778	0.0315769	20	0.631537	2.0	1020

SCALING ANALYSYS

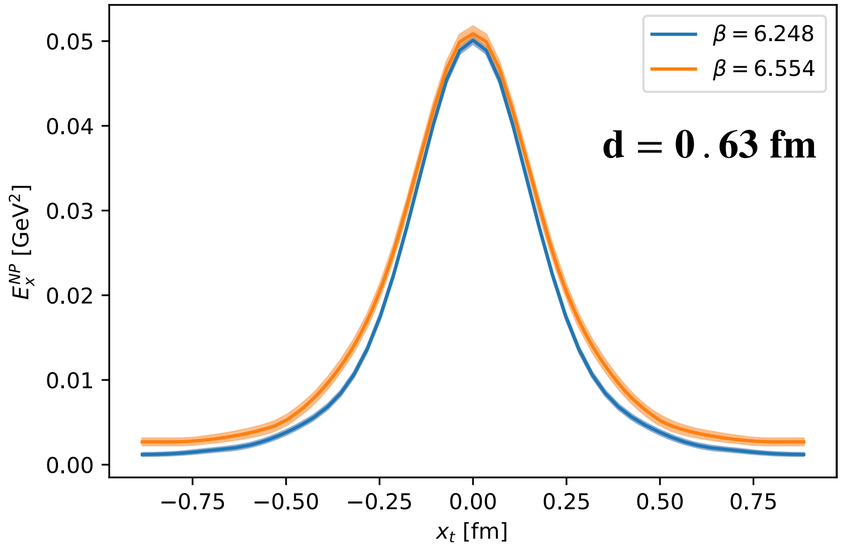

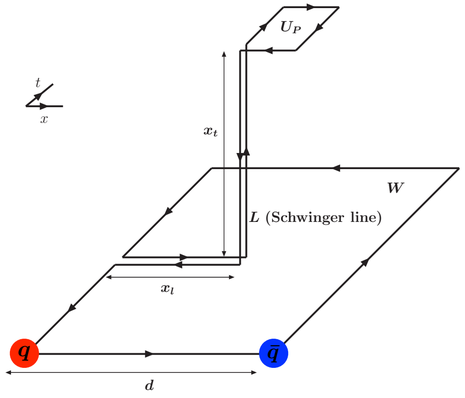

$$T = \frac{1}{a(\beta)\, N_t} \qquad T_c = 260\,\text{MeV}$$

Measurement of the chromoelectric field using the maximal Wilson loop (i.e. the loop with the largest possible extension in the temporal direction).

O. Jahn, O. Philipsen, Phys. Rev. D 70, 074504 (2004). arxiv:hep-lat/0407042

e.g.: lattice $48^3 \times 12$ and distance $d = 15a$ between the sources —> Wilson loop $15(\text{space}) \times 12(\text{time})$

The nonperturbative chromoelectric field

Full profile of the chromoelectric field

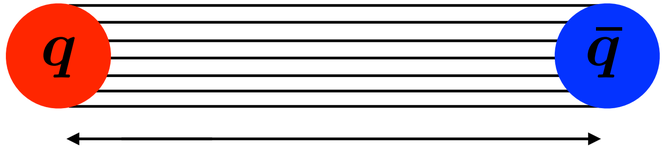

$$d = 0.631\ \text{fm}$$

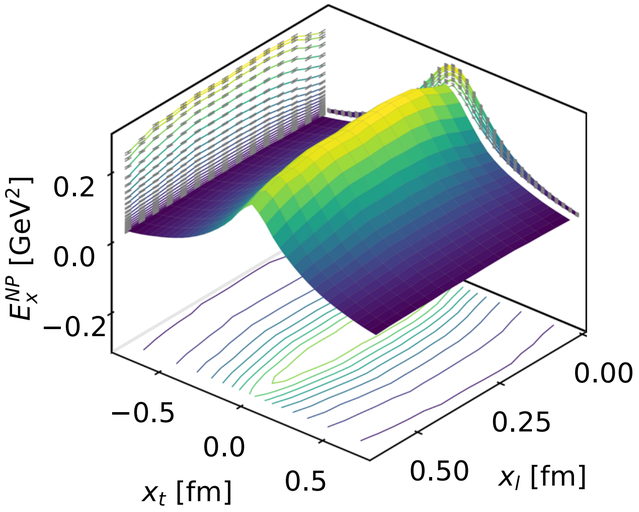

$$T = 0$$

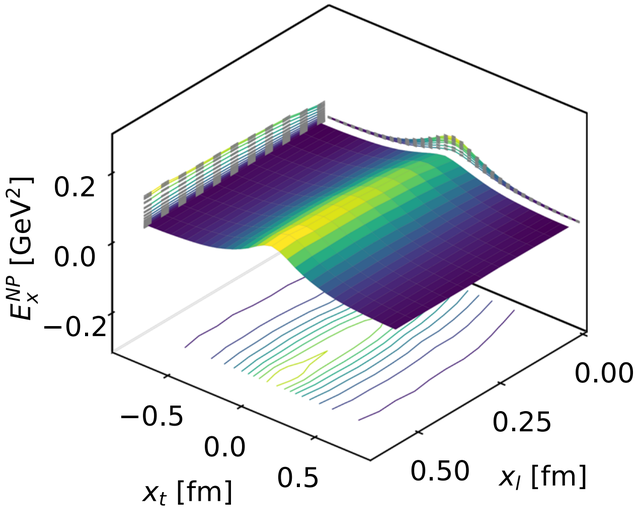

$$T = 1.2\,T_c$$

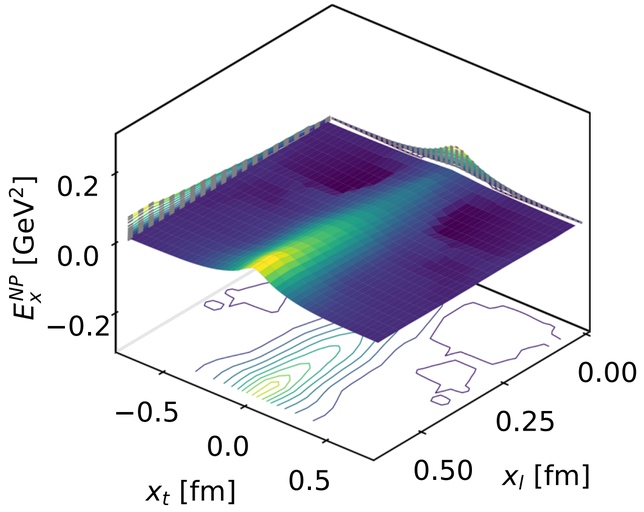

$$T = 2.0\,T_c$$

The chromoelectric field continues to form a tube-like structure well after reaching the deconfinement temperature, despite the values becoming much smaller at higher temperatures.

The chromoelectric field at the midplane between the sources

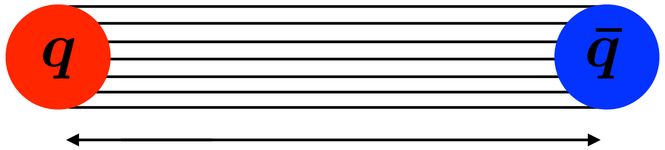

$$d = 0.632\,\text{fm}$$

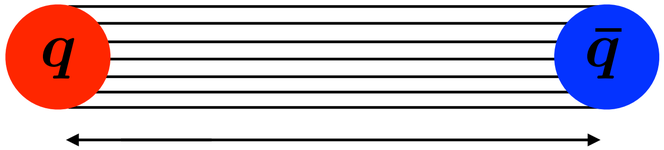

$$d = 0.632\,\text{fm}\,, \quad d = 0.842\,\text{fm}$$

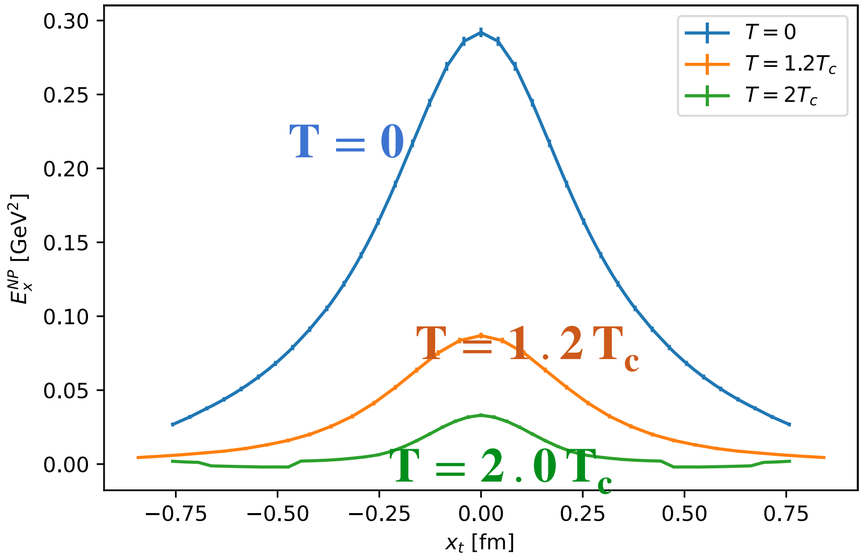

The nonperturbative chromoelectric field at the midplane: providing a better view of the flux-tube remnant evaporation at $T > T_c$

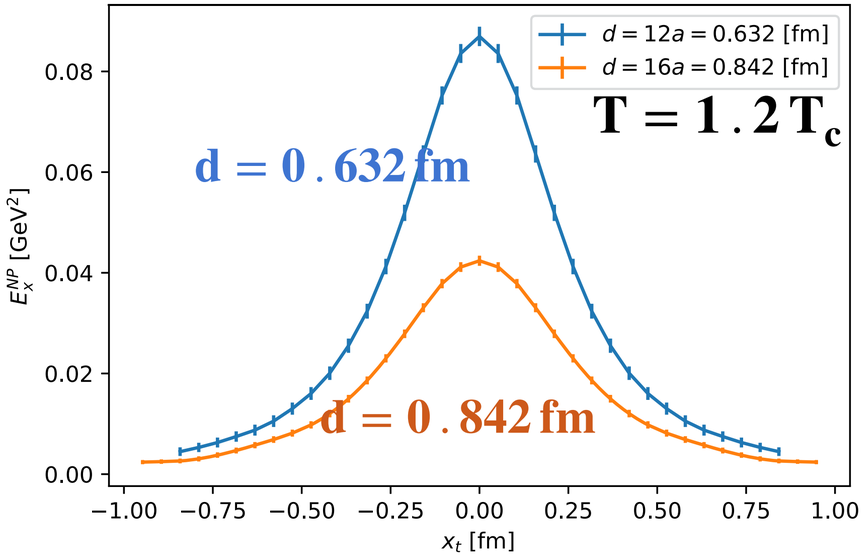

When the quark-antiquark separation is increased by 1/3, the field values fall by more than 50 %, and thus the flux-tube remnant does not create a linear potential at large distances.

The effective string tension

$$\sigma_{\text{eff}} = \int d^2x_t \, \frac{(E_x^{\text{NP}}(x_t))^2}{2}$$

numerical evaluation of the integral using the data for the nonperturbative chromoelectric field at the midplane

β	d [fm]	T/T_c	x_l [fm]	$x_{t,\max}$ [fm]	$\sqrt{\sigma_{\text{eff}}}$ [GeV]
6.240	0.511	0	0.032 – 0.415	1.022	0.4742(15)
6.544	0.511	0	0.021 – 0.448	0.511	0.4692(23)
6.769	0.511	0	0.016 – 0.463	0.511	0.467(7)
6.554	0.631	0	0.021 – 0.610	0.736	0.487(6)
6.100	0.947	0.8	0.039 – 0.829	1.144	0.535(20)
6.381	0.632	1.2	0.026 – 0.553	0.818	0.129(4)
6.381	0.842	1.2	0.026 – 0.816	0.921	0.0733(25)
6.554	0.631	1.5	0.021 – 0.610	0.736	0.0625(19)
6.248	0.632	1.5	0.032 – 0.600	0.853	0.0556(8)
6.778	0.632	2.0	0.016 – 0.616	0.742	0.0305(14)

$T < T_c$

$T > T_c$

The decrease of the values of the integrals above the phase transition is a sign of the flux tube dissolution.

QCD (2+1) flavors at $T = 0$

LATTICE SETUP

- Simulation of lattice **QCD with 2+1 flavors of HISQ (Highly Improved Staggered Quarks) quarks**, with the tree level improved Symanzik gauge action (HISQ/tree).

- Couplings are adjusted so as to move on a **line of constant physics** (LCP), as determined in Bazavov et al (arXiv:111.1710) with the strange quark mass m_s fixed at its physical value and a light-to-strange mass ratio $m_l/m_s = 1/20$, corresponding to a **pion mass of 160 MeV** in the continuum limit.

- We fix the **lattice spacing** through the observable r_1 as defined in Bazavov et al (arXiv:111.1710)

$$\frac{a}{r_1}(\beta)_{m_l=0.05m_s} = \frac{c_0 f(\beta) + c_2(10/\beta) f^3(\beta)}{1 + d_2(10/\beta) f^2(\beta)}$$

$$c_0 = 44.06,\ c_2 = 272102,\ d_2 = 4281,\ r_1 = 0.3106(20)\ \text{fm}$$

- **MILC code** for producing **gauge configurations** (1 saved after 25 RHMC trajectories) and for the measurements of the chromoelectromagnetic field tensor. **Simulations on LEONARDO@Cineca.**

- **Smoothing of gauge configuration:** 1HYP on temporal links + n HYP3d on space links.

SUMMARY OF THE NUMERICAL SIMULATIONS

lattice size	beta	a(beta) [fm]	d [lattice spacings]	d [fm]	#of measurements
48^4	6.885	0.0949777	6	0.569866	500
32^4	7.158	0.0738309	8	0.590647	10064
24^4	6.445	0.144692	5	0.723462	3330
32^4	7.158	0.0738309	10	0.738309	10181
48^4	6.885	0.0949777	8	0.75982	779
32^4	6.885	0.0949777	8	0.759821	4409
32^4	6.5824	0.126658	6	0.759947	2667
32^4	6.3942	0.15203	5	0.760151	3000
32^4	6.885	0.0949777	9	0.854799	4347
32^4	6.25765	0.173715	5	0.868573	3545
32^4	6.5824	0.126658	7	0.886605	2667
32^4	6.3942	0.15203	6	0.912182	3000
48^4	6.885	0.0949777	10	0.949777	779
32^4	7.158	0.0738309	13	0.959801	10183
24^4	6.445	0.144692	7	1.01285	3330
32^4	6.5824	0.126658	8	1.01326	2666
32^4	7.158	0.0738309	14	1.03363	2107
32^4	6.25765	0.173715	6	1.04229	3549
32^4	6.885	0.0949777	11	1.04475	4408
32^4	6.3942	0.15203	7	1.06421	3000
32^4	6.33727	0.160714	7	1.125	3133
32^4	6.885	0.0949777	12	1.13973	4409
48^4	6.885	0.0949777	12	1.13973	769
32^4	6.5824	0.126658	9	1.13992	2667
32^4	6.314762	0.164286	7	1.15	3651
24^4	6.445	0.144692	8	1.157536	3330
32^4	6.28581	0.168999	7	1.18299	3148
32^4	6.25765	0.173715	7	1.216	3546
32^4	6.3942	0.15203	8	1.21624	3000
32^4	6.885	0.0949777	13	1.23471	4409
32^4	6.5824	0.126658	10	1.26658	2667
32^4	6.3942	0.15203	9	1.36827	3000

- **distance between the static sources:**

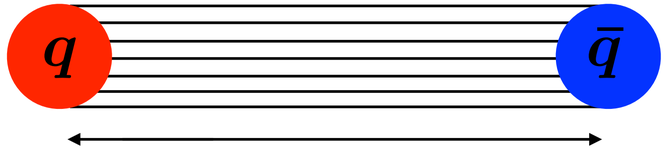

$$0.570 \leq d \leq 1.368 \text{ fm}$$

$$\rho^{\text{conn}}_{W,\mu\nu}$$

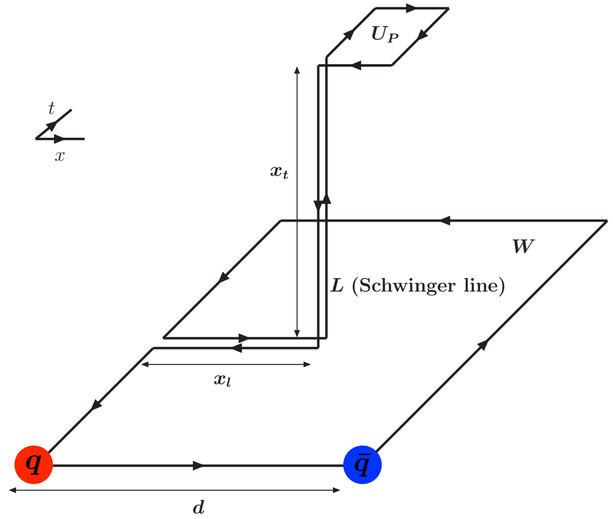

- **Nontrivial renormalization** [N.Battelli, C.Bonati, arXiv:1903.10463] which depends on x_t. By comparing our results we argued that **smearing** behaves as an **effective renormalization.**
- The smearing procedure can also be validated a posteriori by the **observation of continuum scaling.**

QCD (2+1): HYP3D SMEARING

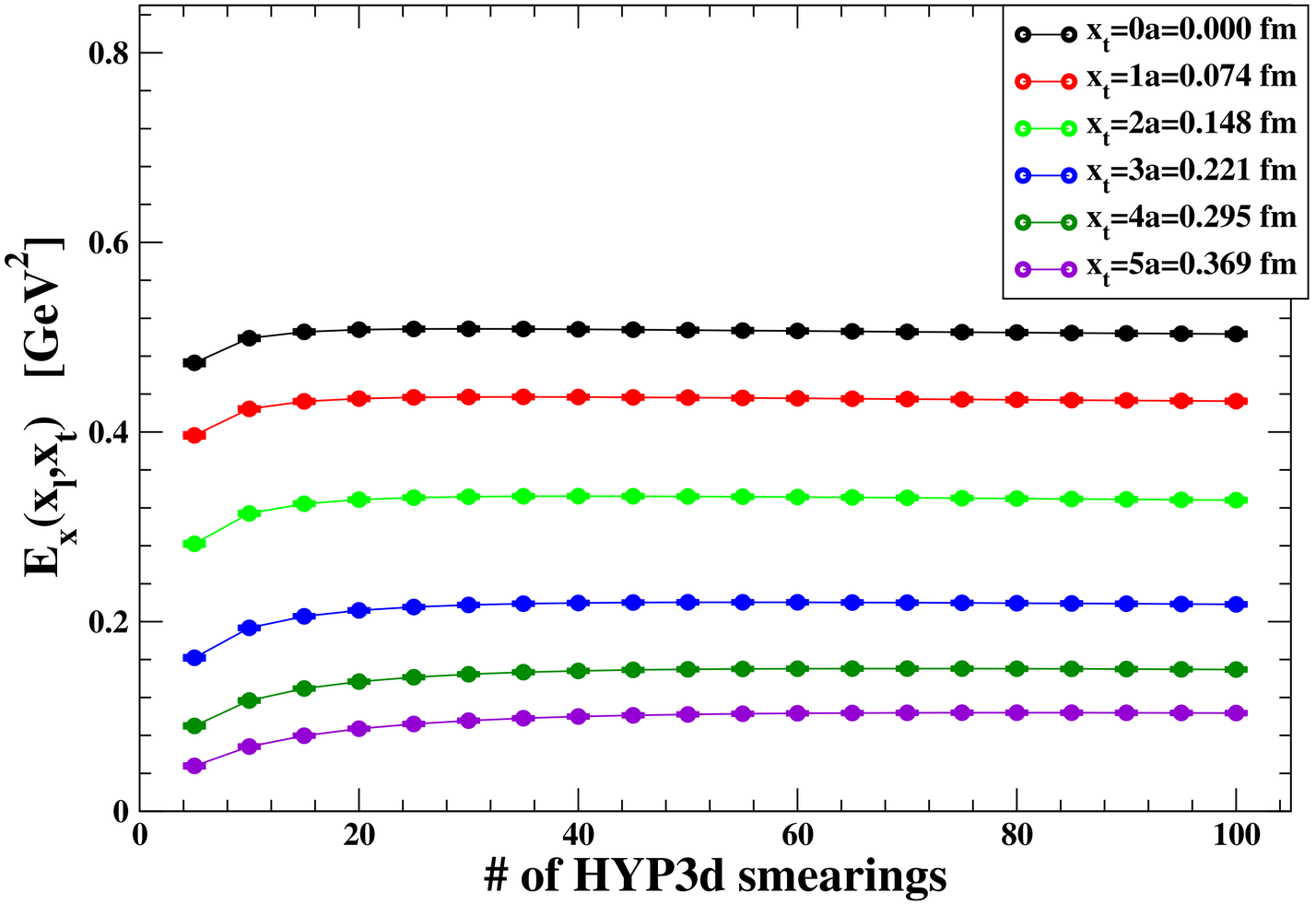

Behavior under smearing of the "full" longitudinal electric field, E_x, for different values of the transverse distance x_t, at $\beta = 7.158$ and $d = 10a = 0.74$ fm on a lattice 32^4.

- The connected correlator exhibits **large fluctuations** at the scale of the lattice spacing, which are responsible for a **small signal-to-noise ratio**.

- To extract the **physical information** carried by fluctuations at the physical scale (and, therefore, at large distances in lattice units), we smoothed out configurations by a **smearing procedure.**

- **Our setup** consists of
  - **one step** of 4-dimensional hypercubic smearing on the temporal links (**HYPt**), with smearing parameters $(\alpha_1, \alpha_2, \alpha_3) = (1.0, 1.0.0.5)$
  - **N steps** of hypercubic smearing (**HYP3d**) restricted to the three spatial directions with $(\alpha_1, , \alpha_3) = (0.75, 0.3)$.

Optimal number of smearing steps: **the field takes its maximum value.**

CONTINUUM SCALING

- We verified that our lattice setup is **close enough to the continuum limit**

by checking that different choices of the lattice parameters, corresponding to the same physical distance **d** between the sources, lead to the same values of the relevant observables when measured in physical units.

$$0.723 \leq d \leq 0.760 \text{ fm}$$

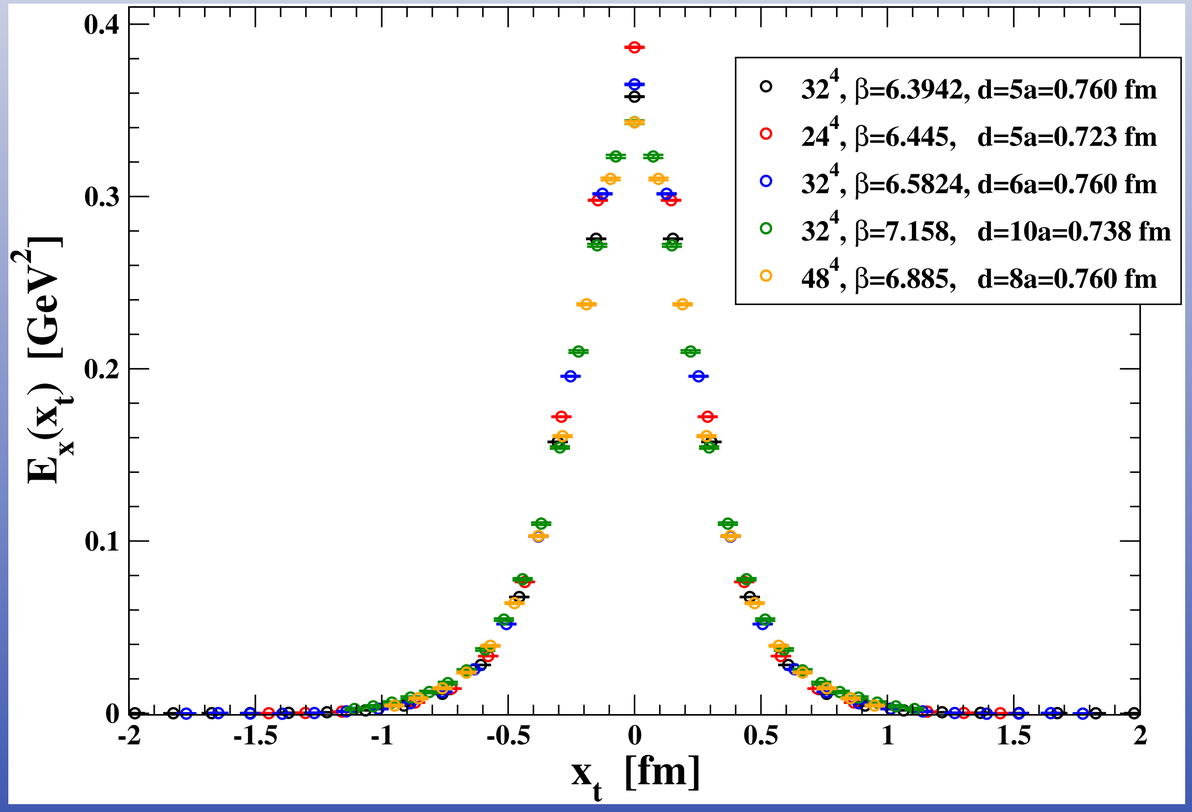

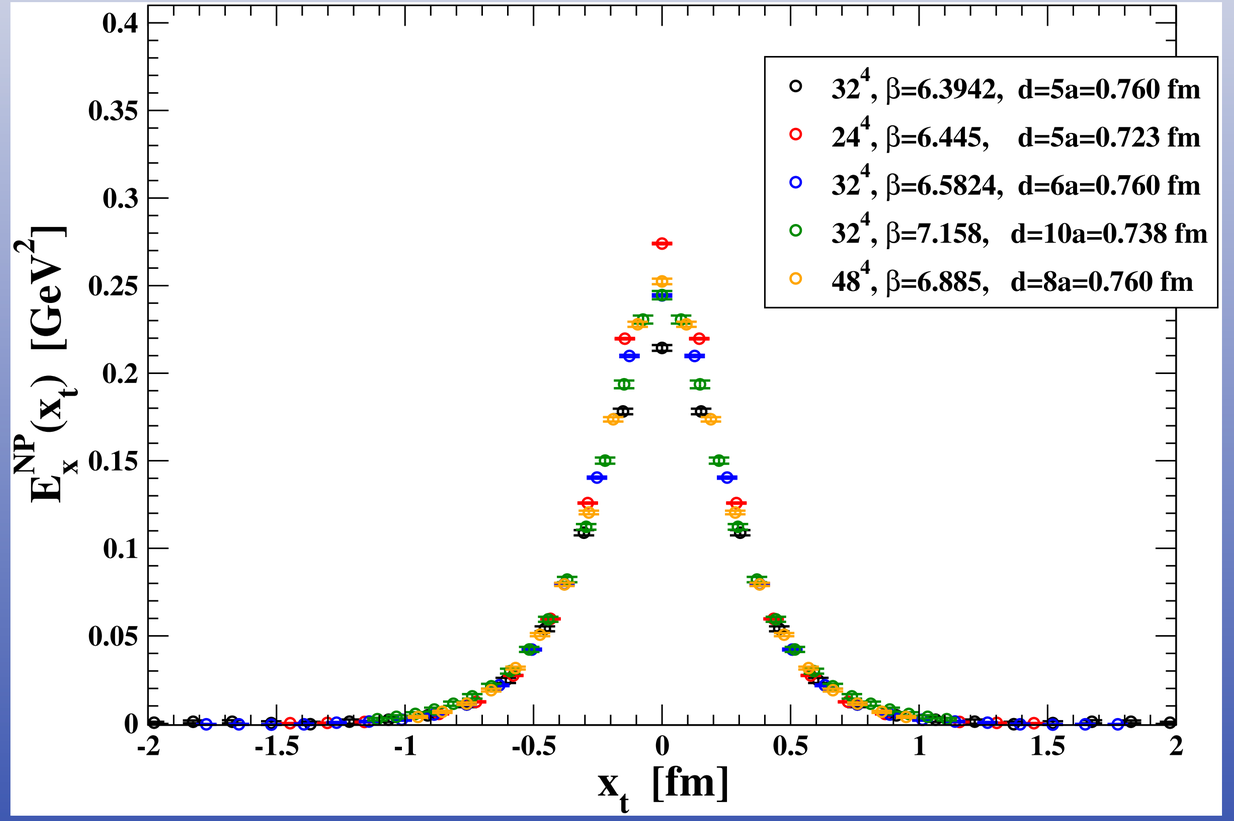

CONTINUUM SCALING (cont'd)

$$0.855 \leq d \leq 0.959 \text{ fm}$$

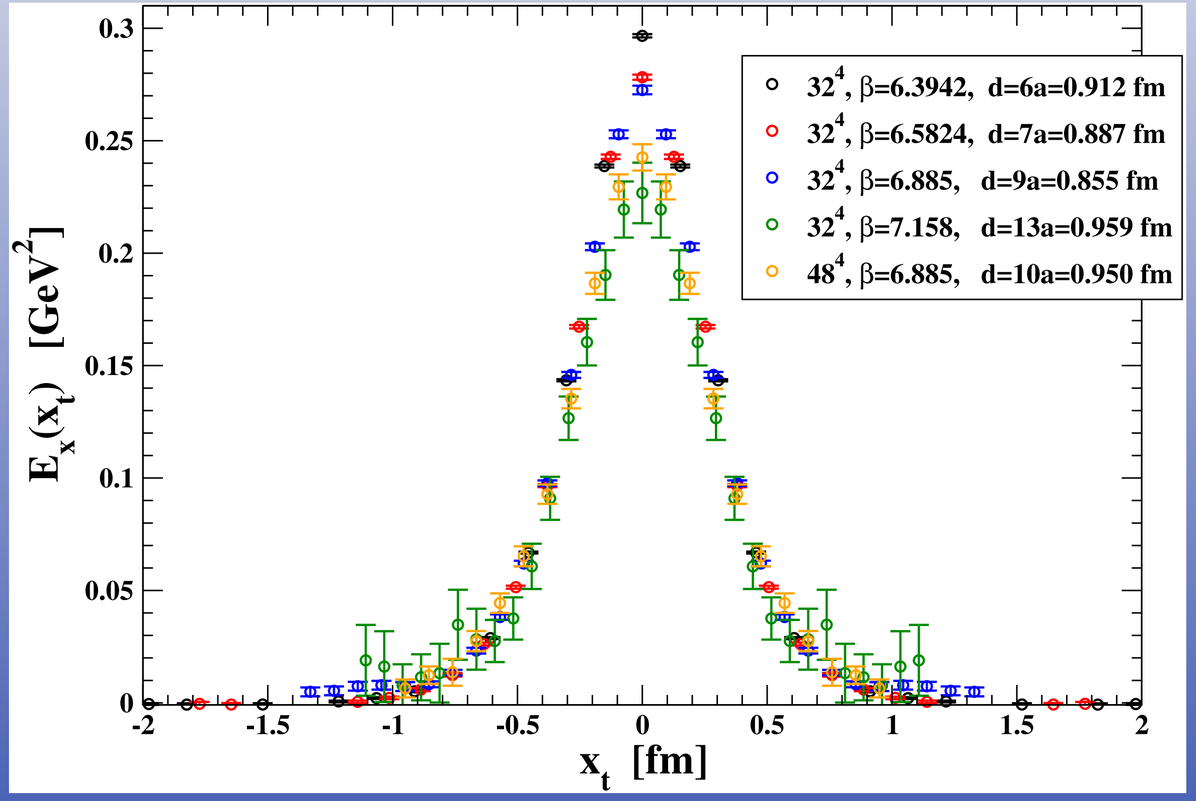

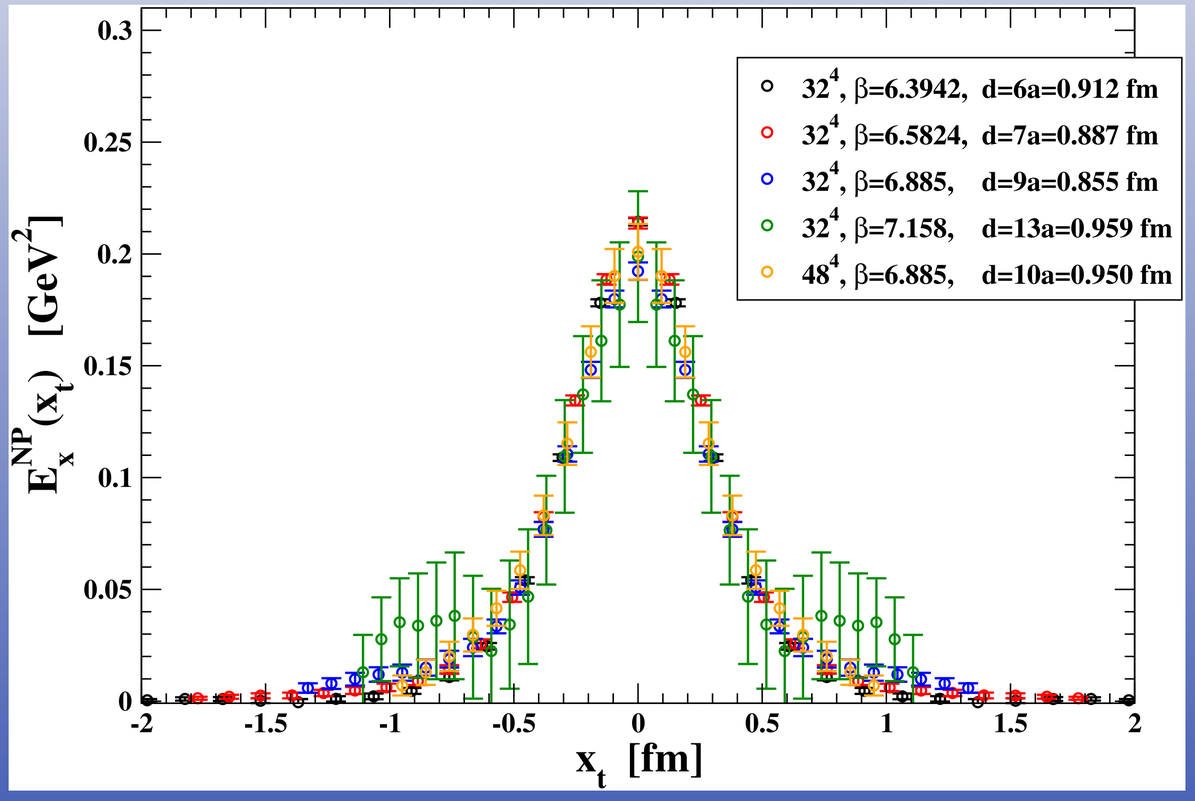

CONTINUUM SCALING (cont'd)

$$1.013 \leq d \leq 1.060 \text{ fm}$$

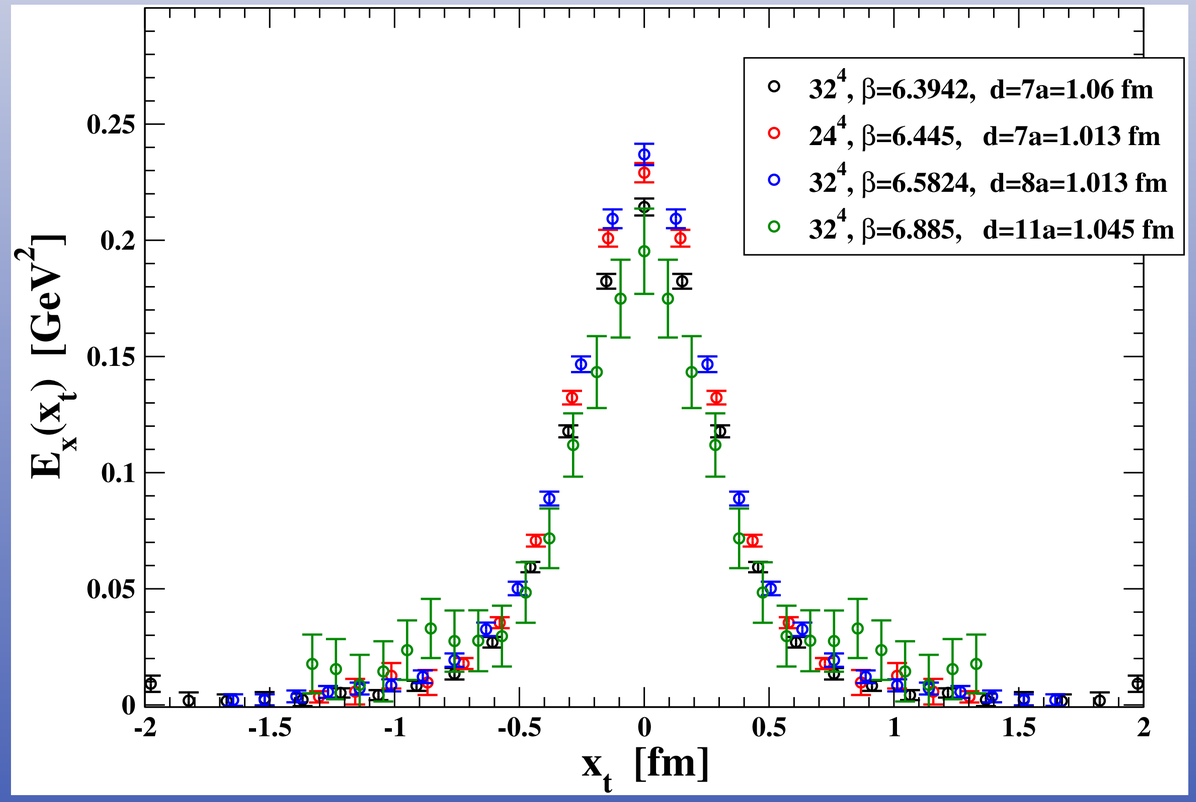

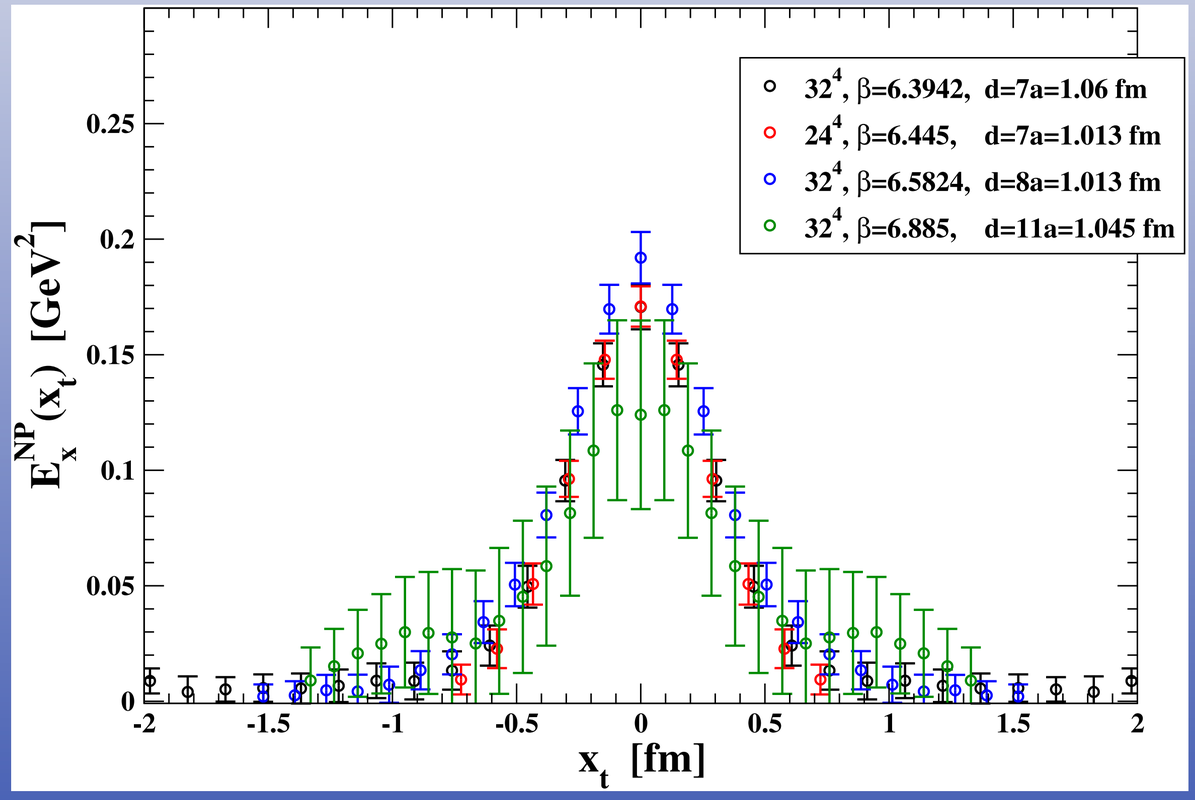

QCD (2+1) flavors: longitudinal chromoelectric field

$$\beta = 7.158 \quad d = 10a = 0.74 \text{ fm}$$

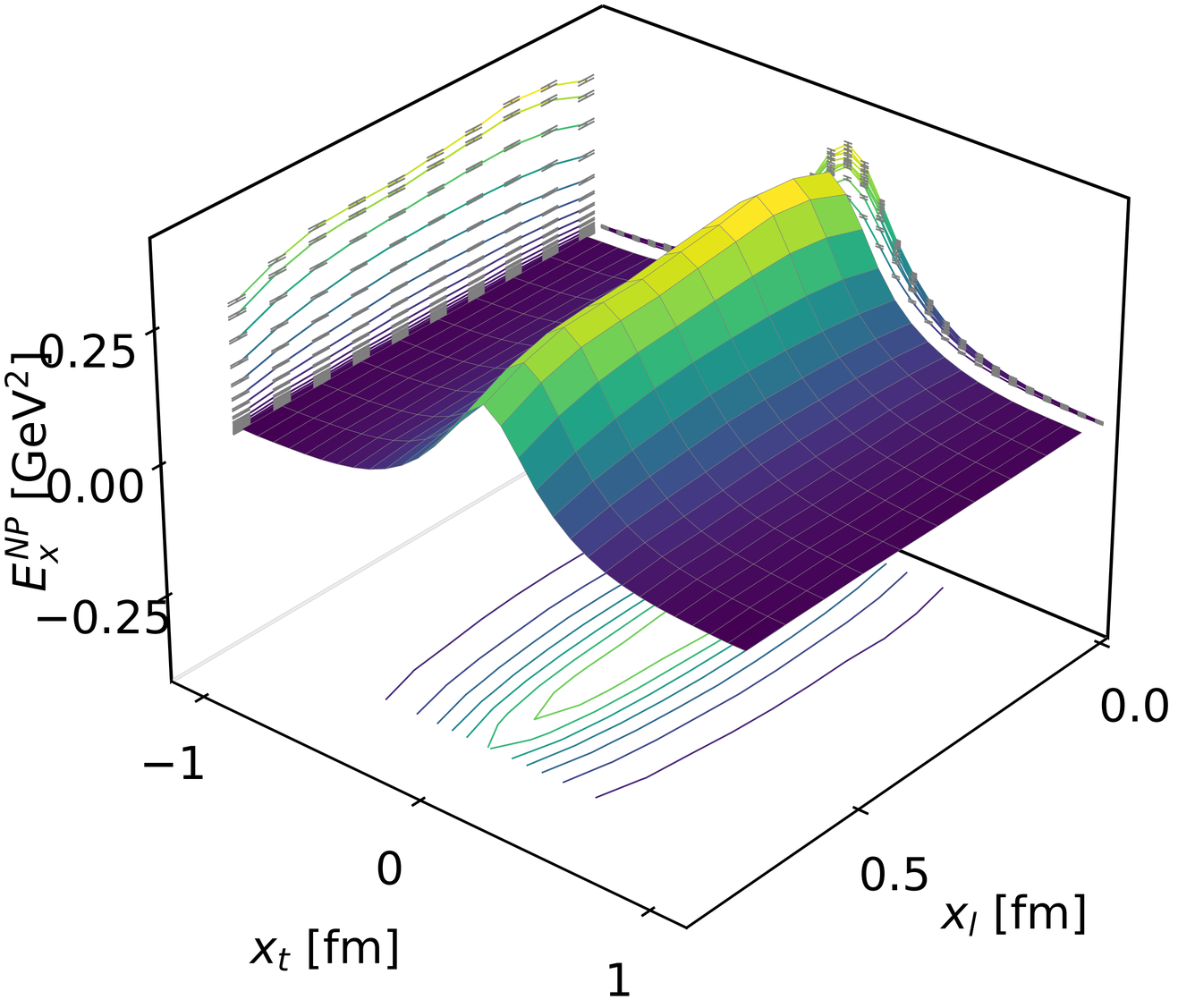

at midplane

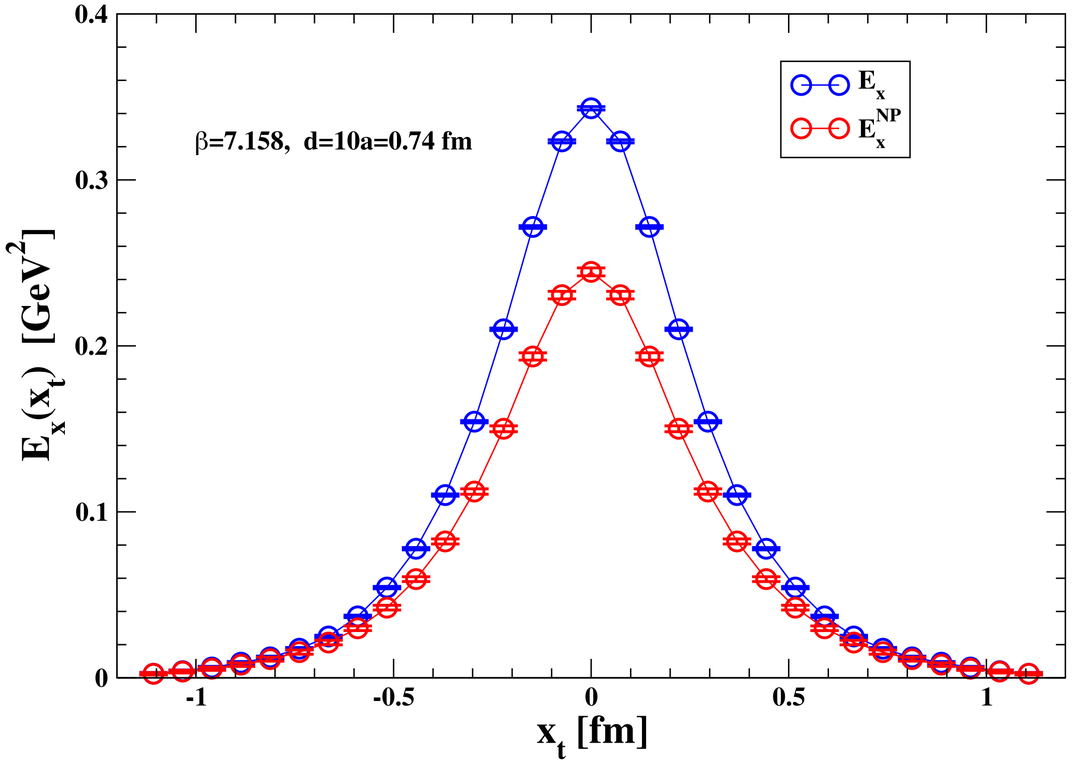

EFFECTIVE STRING TENSION

To characterize quantitatively the **shape** and some **properties of the flux tube** formed by the longitudinal electric field, we calculated numerically (at the midplane between the sources):

$$\sigma_{\text{eff}} = \int d^2x_t \, \frac{(E_x^{NP}(x_t))^2}{2}$$

"effective" string tension

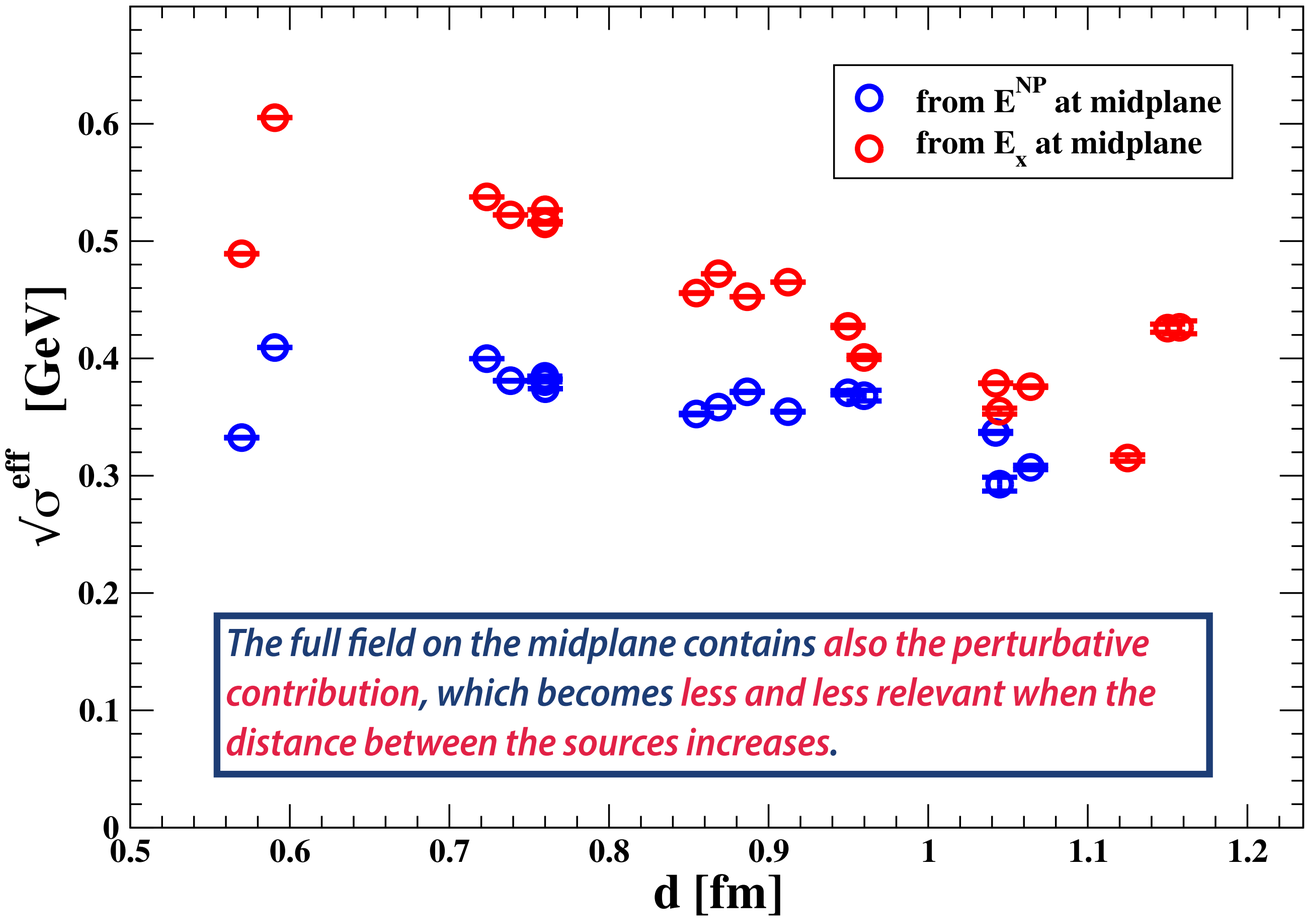

The full field on the midplane contains also the perturbative contribution, which becomes less and less relevant when the distance between the sources increases.

E_x^{NP} at the midplane

d [fm]	$\sqrt{\sigma_{\text{eff}}}$
0.569866	0.332452 (212)
0.590647	0.409334 (58)
0.723462	0.399771 (77)
0.738309	0.380966 (255)
0.75982	0.384704 (187)
0.759821	0.380184 (205)
0.759947	0.382267 (117)
0.760151	0.374200 (68)
0.854799	0.352591 (637)
0.868575	0.358531 (117)
0.886605	0.371464 (449)
0.912182	0.354552 (319)
0.949777	0.370686 (1791)
0.959801	0.368236 (4516)
1.04229	0.336868 (810)
1.04475	0.292763 (5907)
1.06421	0.307063 (1845)

E_x at the midplane

d [fm]	$\sqrt{\sigma_{\text{eff}}}$
0.569866	0.489183 (177)
0.590647	0.605219 (33)
0.723462	0.537672 (46)
0.738309	0.522341 (128)
0.75982	0.514655 (113)
0.759821	0.515571 (100)
0.759947	0.526670 (53)
0.760151	0.516572 (32)
0.854799	0.455681 (282)
0.868575	0.472161 (51)
0.886605	0.452573 (170)
0.912182	0.464997 (124)
0.949777	0.427284 (957)
0.959801	0.400833 (1757)
1.04229	0.378825 (271)
1.04475	0.355045 (2577)
1.06421	0.375906 (586)
1.125	0.315084 (2681)
1.15	0.425761 (3482)
1.157536	0.426480 (5478)

$$\sqrt{\sigma_{\text{eff}}} \approx 0.4 \text{ GeV}$$

WIDTH OF THE FLUX TUBE

To characterize quantitatively the **shape** and some **properties of the flux tube** formed by the longitudinal electric field, we calculated numerically (at the midplane between the sources):

$$w = \sqrt{\frac{\int d^2x_t \, x_t^2 E_x^{NP}(x_t)}{\int d^2x_t \, E_x^{NP}(x_t)}}$$

width of the flux tube

$$w \approx 0.5 \text{ fm}$$

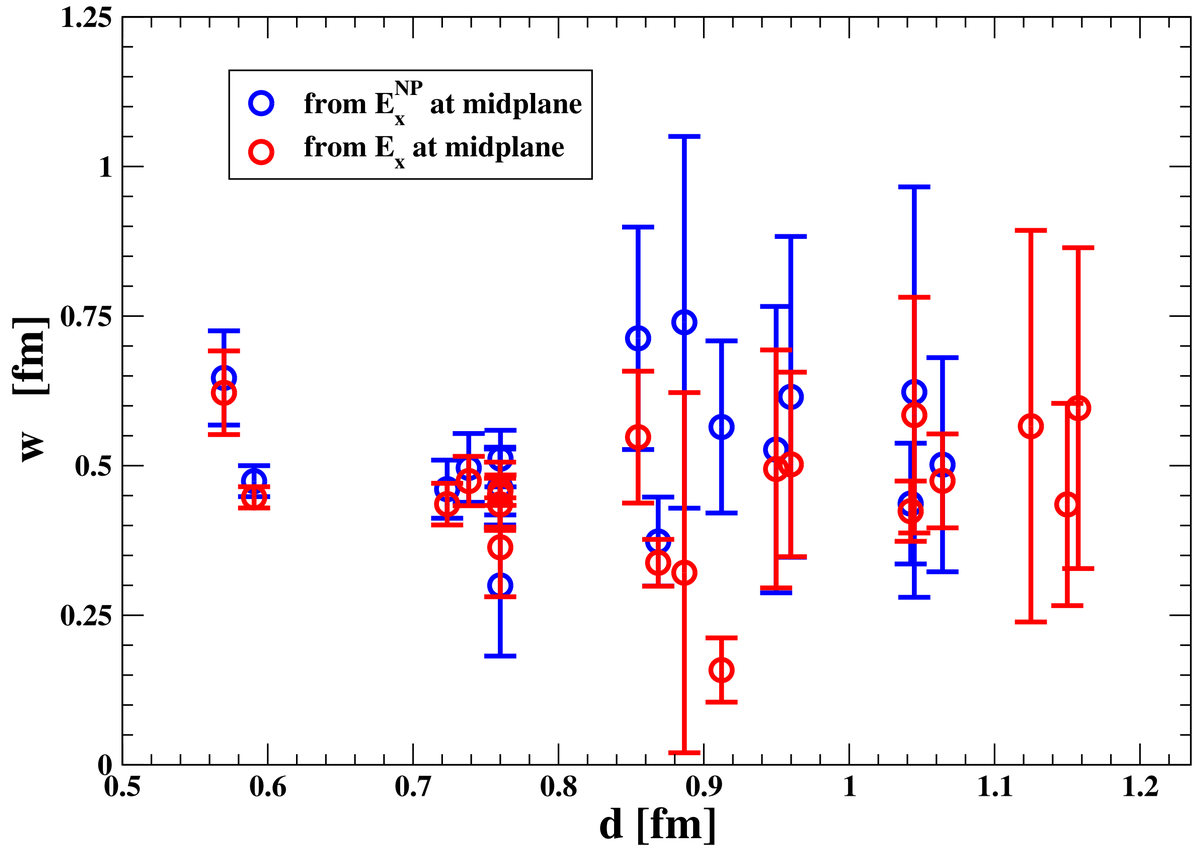

E_x^{NP} at the midplane

d [fm]	w
0.569866	0.646585 (78748)
0.590647	0.474086 (25839)
0.723462	0.460645 (48577)
0.738309	0.496320 (57512)
0.75982	0.463356 (67456)
0.759821	0.464393 (63411)
0.759947	0.299796 (117924)
0.760151	0.511873 (47241)
0.854799	0.712877 (185931)
0.868575	0.373149 (74361)
0.886605	0.739608 (310653)
0.912182	0.564672 (143845)
0.949777	0.526818 (239288)
0.959801	0.614954 (268025)
1.04229	0.436552 (100896)
1.04475	0.622952 (342927)
1.06421	0.501584 (178880)

E_x at the midplane

d [fm]	w
0.569866	0.621870(69886)
0.590647	0.447115(17753)
0.723462	0.435692(34762)
0.738309	0.474240(41283)
0.75982	0.451601(54312)
0.759821	0.435405(43580)
0.759947	0.363556(82688)
0.760151	0.459008(25524)
0.854799	0.547670(110240)
0.868575	0.337704(39088)
0.886605	0.321108(300997)
0.912182	0.158464(53710)
0.949777	0.494548(198891)
0.959801	0.502093(154215)
1.04229	0.423873(50377)
1.04475	0.584496(197020)
1.06421	0.474587(78494)
1.125	0.565908(327225)
1.15	0.435095(169046)
1.157536	0.596161(268178)

the width of the flux tube remains stable on a wide range of distances and is generally compatible for the full and the nonperturbative field.

POSSIBLE EVIDENCE FOR STRING BREAKING

- In the presence of **light quarks** it is expected that the **string between the static quark-antiquark** pair **breaks at large distance** due to ***creation of a pair of light quarks which recombine with the static quarks into two static-light mesons***.

- Usually, the **string breaking distance** is defined as the point where **the Wilson loop and the static-light meson operator have equal overlap onto the ground state**.

Evidences for string breaking:

$N_f = 2, m_\pi = 640\ \mathrm{MeV}$	$d^* = 1.248(13)\ \mathrm{fm}$	Bali et al., hep-lat/0505012
$N_f = 2+1$ **(Wilson)**, $m_\pi = 280\ \mathrm{MeV}$	$d^* \approx 1.216\ \mathrm{fm}$	Kock et al., arXiv/1811.09289
$N_f = 2+1$ **(Wilson)**, $m_\pi \in [200, 340]\ \mathrm{MeV}$	$d^* \approx 1.211(7)\ \mathrm{fm}$	Bulava et al., arXiv/2403.00754

- Our numerical setup is **not tailored for a clear-cut detection** of the expected **string breaking**.

However, **we can look directly at the nonperturbative gauge-invariant longitudinal electric field**, E_x^{NP}, in the region between two static sources that is responsible for the formation of a well-defined flux tube, characterized by nonzero effective string tension σ_{eff} and width w.

POSSIBLE EVIDENCE FOR STRING BREAKING (cont'd)

We tried to push our numerical simulations to distances as large as ~ 1.37 fm, searching for **hints of string breaking**.

- $0.570 \text{ fm} \leq d \leq 1.064 \text{ fm}$ ($d \approx 1.125$ fm under scrutiny)

  We are able to isolate the non perturbative part of the longitudinal electric field

- $1.140 \text{ fm} \lesssim d < 1.368 \text{ fm}$

  We find evidences for the full longitudinal electric field E_x on the midplane between two sources

  BUT

  there are not evidences for a sizeable nonperturbative longitudinal electric field E_x^{NP}.

- For $d > 1.140$ fm

  No improvement in the signal can be observed **if the distance in lattice units between the two sources is reduced**, **keeping d fixed.**

- In **SU(3) pure gauge**, where the string remains unbroken by definition, **the signal for the longitudinal field is clear even at large distances both in physical and lattice units**.

Our preliminary estimate for the string breaking distance is:

$$1.064 \text{ fm} \lesssim d^* \lesssim 1.140 \text{ fm}$$

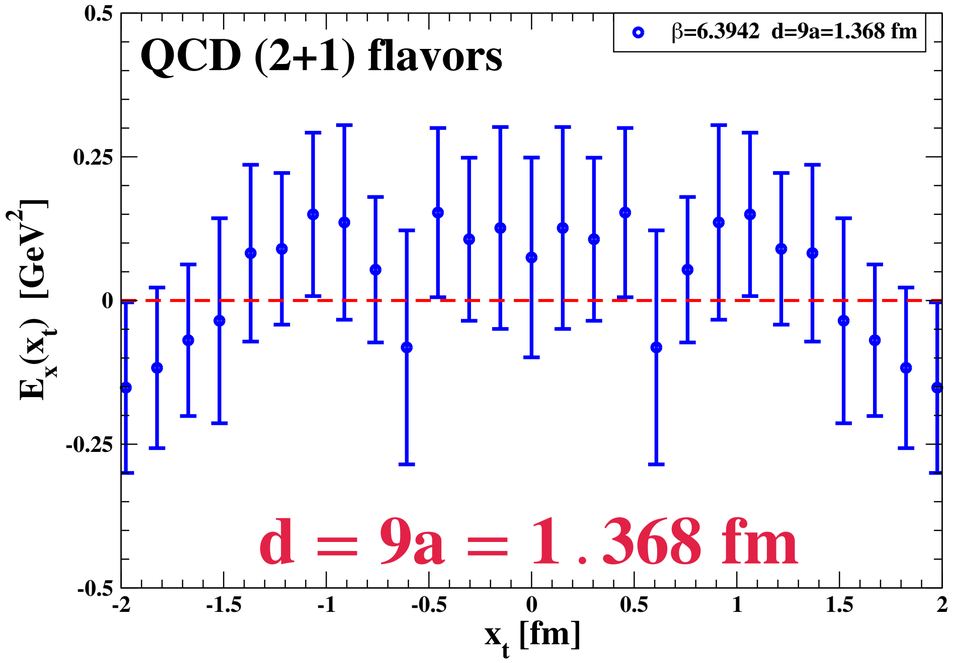

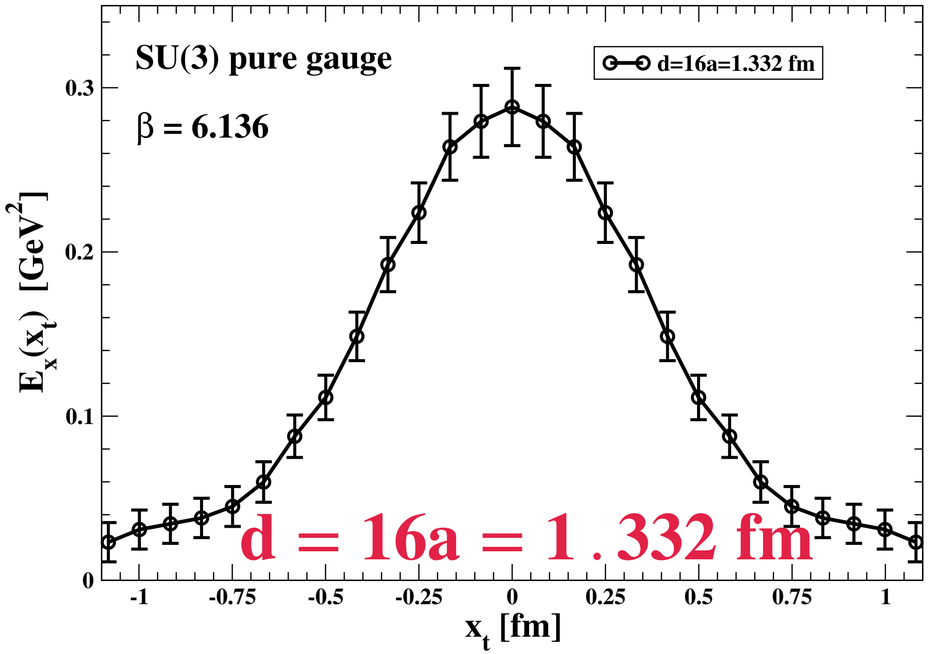

SUMMARY AND CONCLUSIONS

- We have studied the **chromoelectromagnetic field tensor** in the region between a quark and an antiquark through Monte Carlo simulations, both in **SU(3) pure gauge theory** and in **QCD with (2+1) dynamical staggered fermions at physical masses**.

- We can extract the **nonperturbative component** of the longitudinal electric field that is directly related to **confinement**.

- We have demonstrated that the **longitudinal electric field forms a flux tube**.

- This flux tube can be characterized by two quantities: $\sigma_{\rm eff}$ (related to the **string tension**), and the **width** $\mathbf{w}$.

- In **SU(3) pure gauge theory at zero temperature**, we observe a flux tube structure even for relatively large separations of the static quark-antiquark pair.

- In **SU(3) pure gauge theory at finite temperature**, we observe that the flux tube structure begins to dissipate above the deconfinement temperature.

- In the case of **QCD with (2+1) dynamical staggered fermions at physical masses**, we have considered several values of the **physical distance between the sources** $\mathbf{0.57\,fm \leq d \leq 1.37\,fm}$.
  - Above $\mathbf{d \simeq 1.14\,fm}$, the longitudinal nonperturbative field $\mathbf{E_x^{NP}}$ is always compatible with zero, within large numerical uncertainties and we have provided some numerical arguments in favour of a **string breaking distance —>** $\mathbf{1.064\,fm \lesssim d^* \lesssim 1.140\,fm}$
  - We plan to corroborate them with **further investigations**. And we also plan to study QCD flux tubes in presence of background fields at finite temperature and/or at finite density.

THANK YOU FOR YOUR ATTENTION !

"If, in some cataclysm, all of scientific knowledge were to be destroyed, and only one sentence passed on to the next generations of creatures, what statement would contain the most information in the fewest words? I believe it is the *atomic hypothesis* (or the atomic *fact*, or whatever you wish to call it) that *all things are made of atoms—little particles that move around in perpetual motion, attracting each other when they are a little distance apart, but repelling upon being squeezed into one another*. In that one sentence, you will see, there is an enormous amount of information about the world, if just a little imagination and thinking are applied."

Richard P. Feynman

in *The Feynman Lectures on Physics*